



BE S²ECURE

(make) Built Environment Safer in Slow and Emergency Conditions through behavioral assessed/designed Resilient solutions

Grant number: 2017LR75XK

WP 2 – BE and SLOD: SoA, Risks and human behavior

T.2.2 - SoA on SLOD (heat wave and pollution) in BE and their effect on health and wellbeing of its users. Methods for data collection and analysis (on medium/long term datasets). Correlation between pollution and climate data (e.g. wind, rain, fog). Current mitigation solution analysis. Identification of BE features and users' (inappropriate) behaviors modifying SLOD effects/risk levels. Development of indicators and relative weights for selected SLOD risk levels assessment

DELIVERABLE ID	D.2.2.1
Deliverable Title	Climate data collection and analysis report
Delivery month	M6
Revision	1.0
Main partner	POLIMI
Additional partners	
Authors of the contribution	Graziano Salvalai; Nicola Moretti, Juan Diego Blanco Cadena, Fulvio Re Cecconi (POLIMI)
Deliverable type	report/report with software documentation/report on dissemination activities/report on coordination activities
Number of pages	32

Abstract

Slow Onset Disasters (SLOD) are responsible for the production of systemic effects on the urban ecosystem and can seriously harm people to be living in the cities. Therefore, the agents underpinning the SLODs must be carefully analysed to acquire a good knowledge of the effects that they may produce on the citizens and investigating how these agents are related to the Built Environment (BE) characteristics. Abnormal weather parameters may produce severe effects on SLODs and especially if combined with air pollution in dense BE could worsen the negative impact on citizens. This report presents a set of analyses carried out on the Lombardy region's open data. These analyses allow to identify the trends of the weather conditions in the BE. For the city of Milan, the temperature, precipitation level, relative humidity, and global horizontal radiation have been analysed from 2016 to 2019. Scaling down the analyses to the case study area, the Universal Thermal Climate Index (UTCI) has been calculated, focusing on the nearest weather central to the case study. This index allows to evaluate the outdoor comfort condition over the considered period of analysis and in different hours of the day. Eventually, weather data have been combined in a risk indicator allowing to assess their compound effect on citizens. The report concludes summarizing the results of the analyses and providing a brief insight on the joint trends of weather data and main air pollutants. However, more in-depth analyses on air pollutants are presented in the D2.2.2.

Keywords

Slow-Onset Disasters, Built Environment; Urban Heat Island; Climate change; Weather data; Universal Thermal Climate Index; Open data

Approvals



BE S²ECURE

(make) Built Environment Safer in Slow and Emergency Conditions through behavioral assessed/designed Resilient solutions

Grant number: 2017LR75XK

Role	Name	Partner
Coordinator	Enrico Quagliarini	UNIVPM
Task leader	Graziano Salvalai	POLIMI

Revision versions

Revision	Date	Short summary of modifications	Name	Partner
0.1	15.04.2020	Minor revision	Enrico Quagliarini	UNIVPM
			Michele Lucesoli	UNIVPM
1.0	17.04.2020	Proofreading and solving of minor comments	Graziano Salvalai	POLIMI
			Enrico Quagliarini	UNIVPM

Summary

1. Introduction
 - 1.1 Identification and selection of weather stations
 - a. Weather data availability
 - 1.2 Insights on potential thermal sensation perceived by inhabitants
 - a. Air temperature
 - b. Precipitation and relative humidity
 - c. Wind velocity
 - d. Global horizontal radiation
 - e. Variations related to the built environment
2. Implications on the selected area in Città Studi
 - 2.1 Distribution frequency function
 - a. Air temperature
 - b. Relative humidity
 - c. Wind velocity
 - d. Incident radiation
 - 2.2 Inhabitants thermal sensation
 - a. Confluence of risk conditions



BE S²ECURE

(make) Built Environment Safer in Slow and Emergency Conditions through behaviorally assessed/designed Resilient solutions

Grant number: 2017LR75XK

-
- b. UTCI
 - 2.3 Indoor air conditioning effects
 - 3. Conclusions
 - 4. References

BE S²ECURE - DRAFT

1. Introduction

Based on the deductions and decisions made throughout D.2.1.1 and D.2.1.2, the following work has concentrated on assessing the SLOD's risk of *Increasing temperatures* and *Air pollution*, on the city of Milan, Lombardy, Italy. This report provides an exhaustive set of analyses accomplished on climate data collected by weather centrals in the city of Milan.

Therefore, the work hereby describes the identification of risk conditions linked to *Increasing temperatures*, while giving few insights on scenarios that might be overlapped with poor air pollution management.

1.1 Identification and selection of weather stations

Within Milan, there are 10 active weather stations that belong to the ARPA (Agenzia Regionale per la Protezione dell'Ambiente) open-source database (ARPA Lombardia). This can be used for gathering information about how the inherent microclimate conditions are progressing. Figure 1 displays how are these stations distributed in the city, and Table 1 shows the information type and identification number of the sensors held in each of the stations.

a. Weather data availability

Recalling the deductions made on D.2.1.1, *increasing temperatures* was considered amongst the SLOD's of greater impact and recurrence. Table 1 allowed to identify only 5 weather stations which host sufficient data to recognize its evidence:

- Milano P.zza Zavattari (M3),
- Milano Lambrate (M1),
- Milano v. Marche (M8),
- Milano v. Juvara (M7), and
- Milano v. Brera (M4).

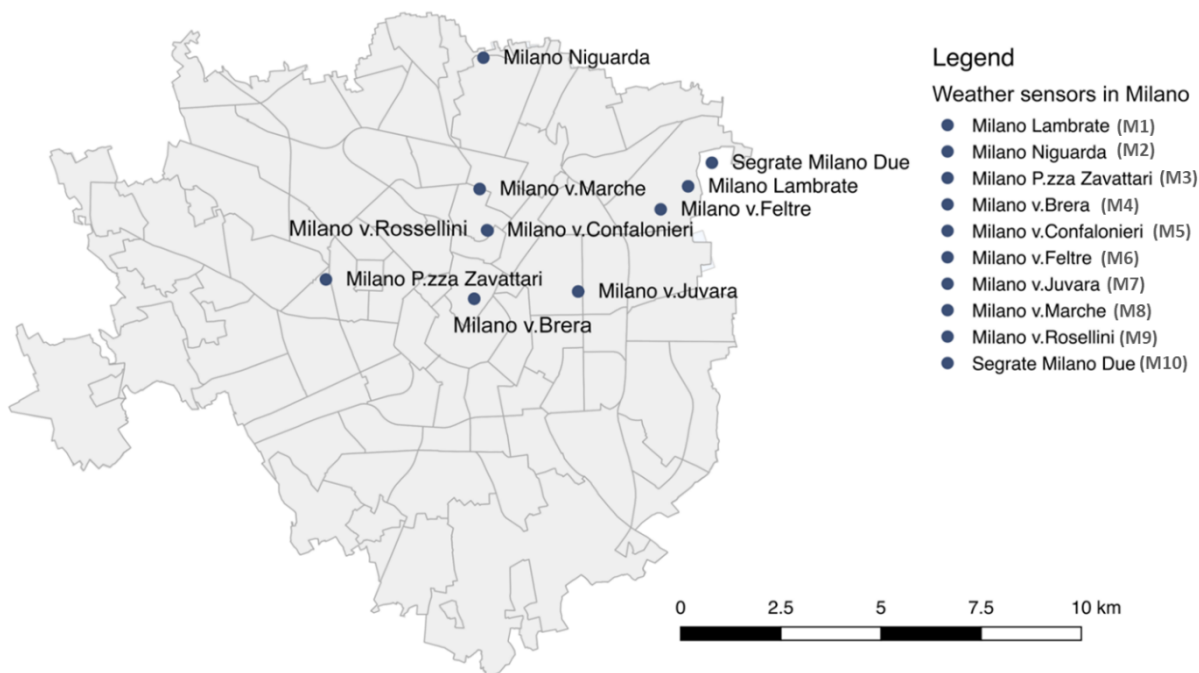


Figure 1: Location of ARPA's weather stations' in Milan (extracted and edited from D.2.1.2).



BE S²ECURE

(make) Built Environment Safer in Slow and Emergency Conditions through behaviorally assessed/designed Resilient solutions

Grant number: 2017LR75XK



Figure 2: Location and context surrounding of ARPA's weather stations¹ in Milan.

Station	Sensor code	Type of sensor
Milano Lambrate	2006	Precipitation
	2001	Temperature
	2002	Relative humidity
	2008	Global radiation
	14391	Wind speed
	14390	Wind direction
Milano Niguarda	3118	Hydrometric level
Milano P.zza Zavattari	5920	Temperature
	19005	Wind speed
	19006	Wind direction
	6185	Relative humidity
	9341	Precipitation
Milano v. Brera	19008	Wind speed
	19374	Global radiation
	5897	Temperature
	19373	Precipitation
	19009	Wind direction
	6174	Relative humidity
Milano Confalonieri	8149	Precipitation
Milano v. Feltre	8125	Hydrometric level
	8162	Temperature
Milano v. Juvara	19244	Wind direction
	5908	Precipitation
	19243	Wind speed



BE S²ECURE

(make) Built Environment Safer in Slow and Emergency Conditions through behavioral assessed/designed Resilient solutions

Grant number: 2017LR75XK

	5909	Temperature
	6179	Relative humidity
	6458	Global radiation
Milano v. Marche		
	6597	Relative humidity
	19020	Wind speed
	5911	Temperature
	19021	Wind direction
Milano v. Rosellini		
	14121	Precipitation
Segrate Milano Due		
	2064	Relative humidity
	2065	Precipitation
	2063	Temperature

Table 1: ARPA stations in Milano, hosted sensor type reading parameter (extracted from D.2.1.2).

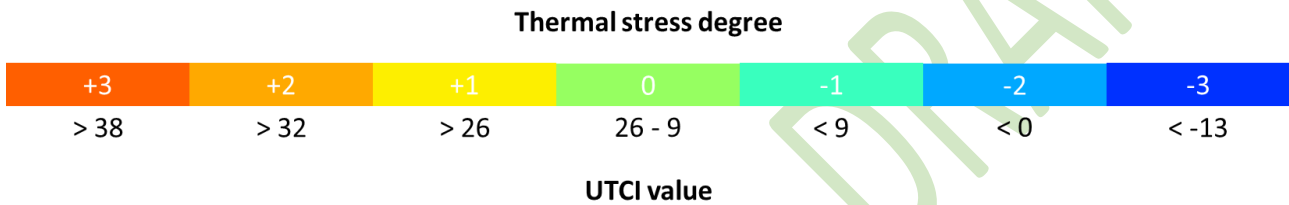


Figure 3: UTCI degree of thermal stress legend.

Therefore, only these stations were assessed for having a preliminary broad knowledge of the city's thermal stress distribution. Initially, all the parameters have been analyzed separately and plotted, as done in

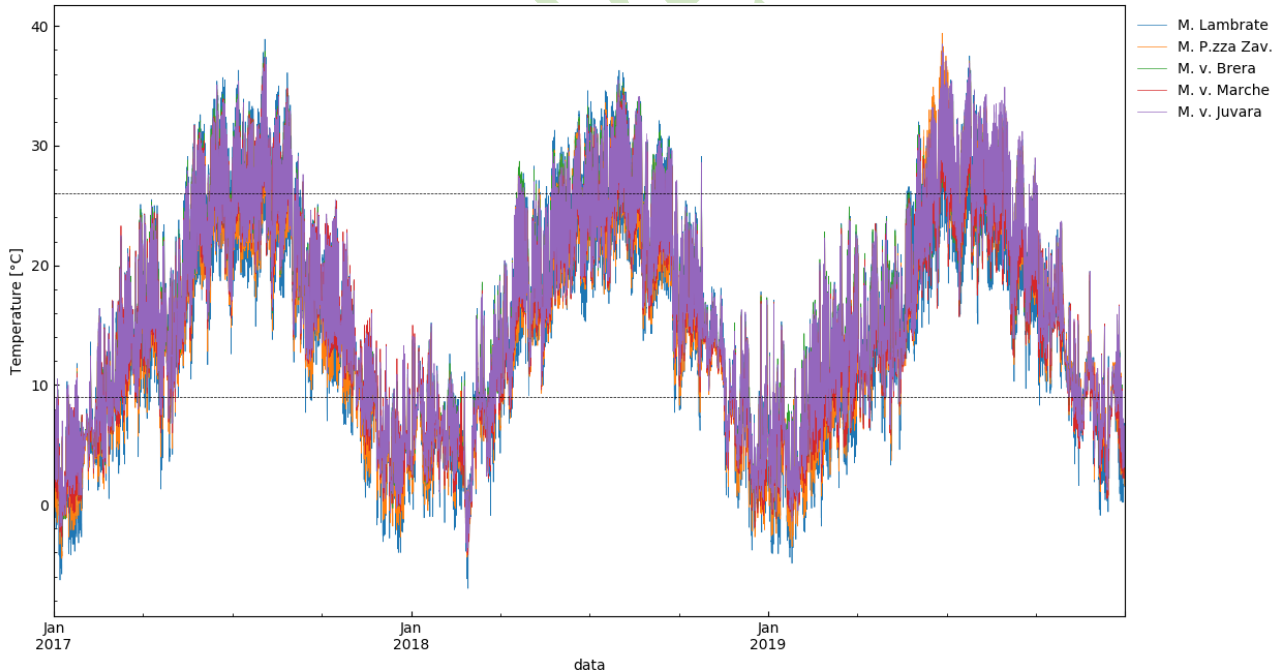


Figure 4 and Figure 5 for air temperature, at an hourly-average and daily-average time-step. Then, thermal perception of people has been estimated, based on an average human body, as a combination of temperature, humidity and wind speed using the definition of Universal Thermal Climate Index (UTCI) (Bröde et al. 2009) (Figure 3).

1.2 Insights on potential thermal sensation perceived by inhabitants

This section describes the potential thermal sensation perceived by inhabitants, according to the weather parameters, retrieved and analyzed thanks to available data from the five selected weather stations in Milano.

a. Air temperature

In

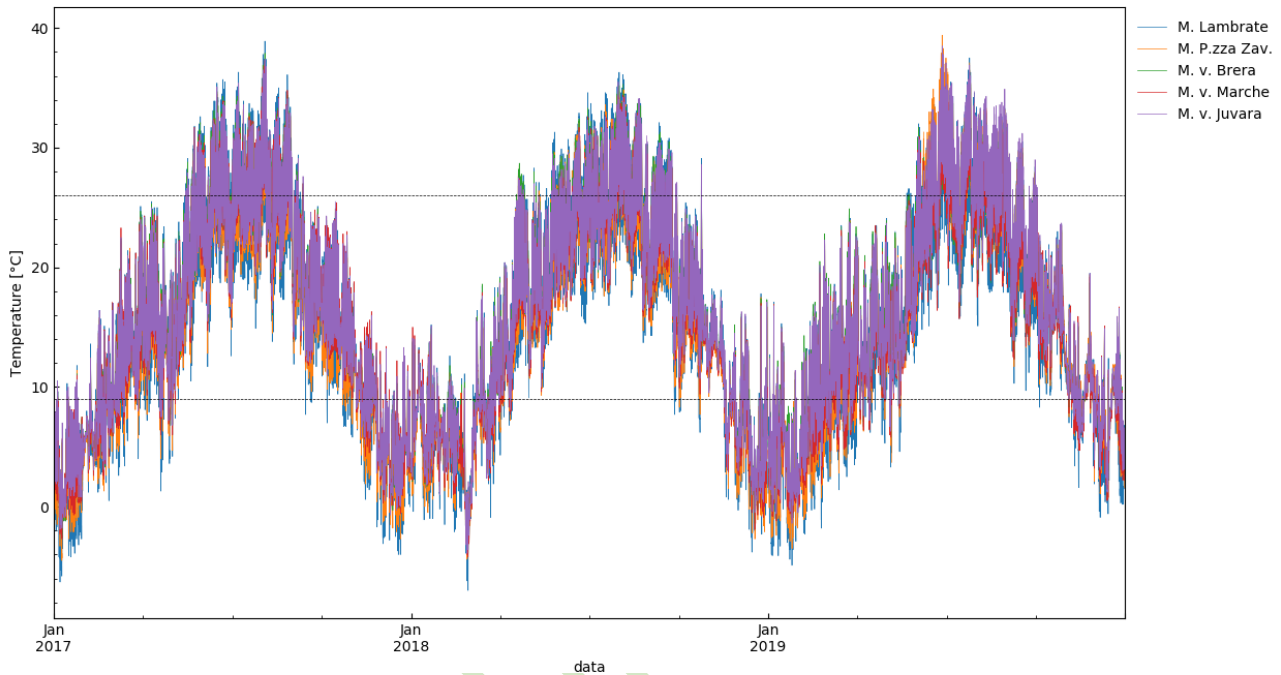


Figure 4, all weather stations, in the period January 2017 – December 2019, seem to have displayed a rather similar trend, except for punctual lower temperature values. However, it is noted that there is a slightly wider air temperature values shift on *Milano Lambrate and M. P.zza Zavattari* station (i.e. Higher and lower air temperature values recorded). The same can be stated for the analysis represented in Figure 5, despite the granularity is different (hourly average vs daily average temperature).



BE²SECURE

(make) Built Environment Safer in Slow and Emergency Conditions through behavioral assessed/designed Resilient solutions

Grant number: 2017LR75XK

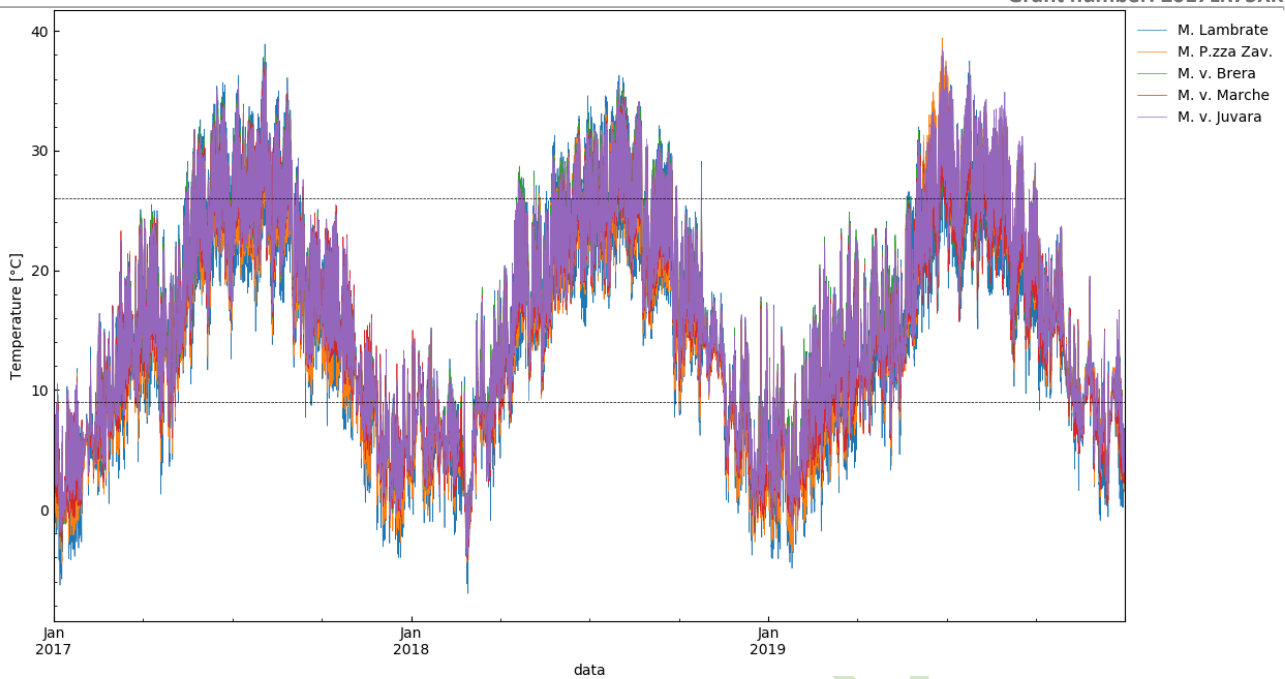


Figure 4: Hourly average of air temperature readings for selected weather stations. Dotted lines demark heat stress thresholds for warm and cold settings according to the UTCI definition (9 and 26 °C).

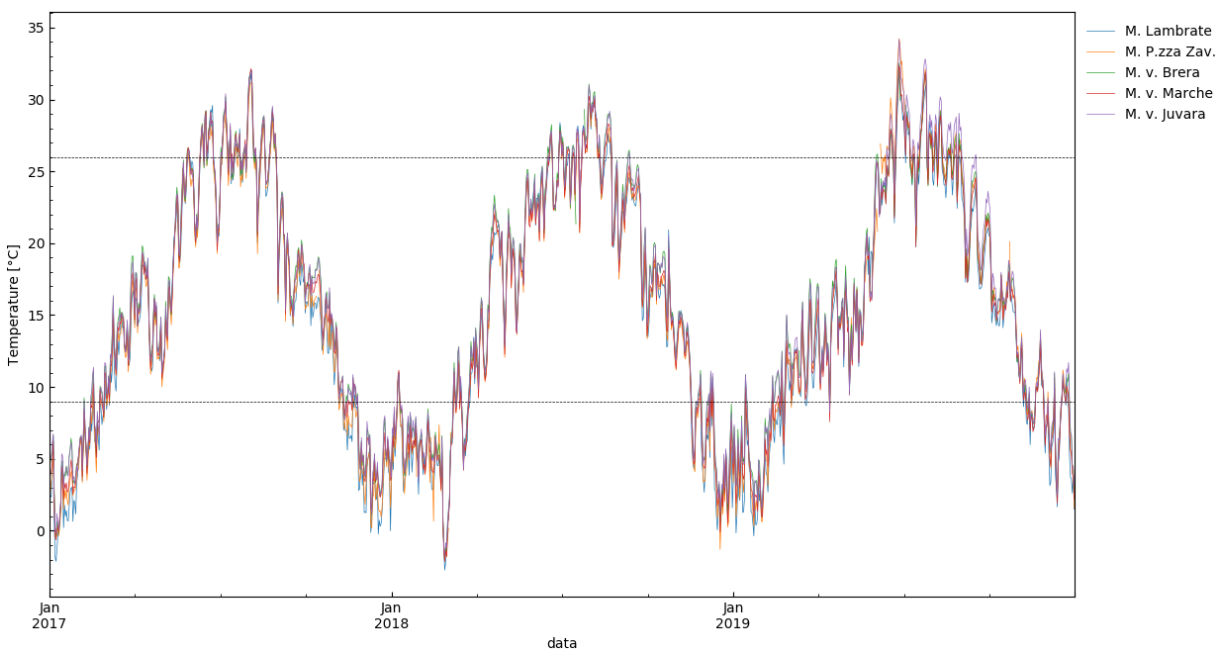
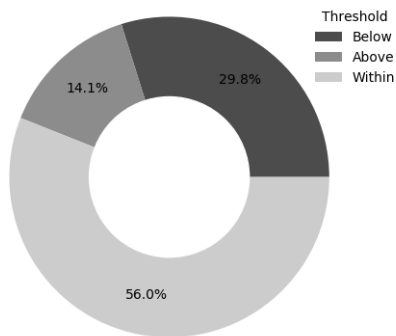


Figure 5: Daily average of air temperature readings for selected weather stations. Dotted lines demark heat stress thresholds for warm and cold settings according to the UTCI definition (9 and 26 °C).

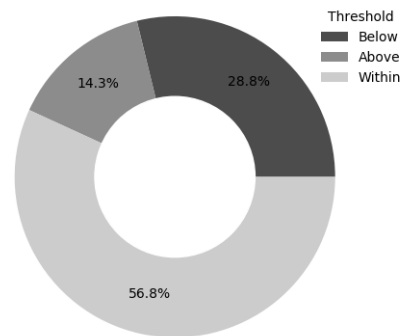
Moreover, in Figure 6 it is noted that for most of the readings, the air temperatures are within the comfort threshold limits (9°-26°C). However, more than one quarter of the registered data retrieved from the considered sensors, are below the lower comfort threshold. This values are all referred to winter season and will not be further considered (Figure 4 and Figure 5).

The values above the upper threshold represent 14 – 16 % of the time and are always present on the summer season (Figure 6). These risk condition will prevail only if relative humidity, wind speed and radiation are neglected. These factors might alleviate (in case of high windspeed) or deteriorate the thermal stress, onto a higher UTCI level (Figure 3), therefore the following analysis are highly relevant.

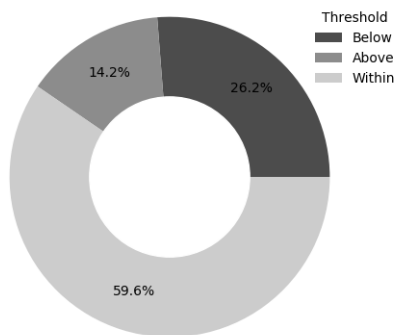
For a greater understanding, Figure 7 has been elaborated, offering a further representation of the hourly-average temperatures, during the day (x axis), from 2016 to 2018. Dark red bars represent missing data.



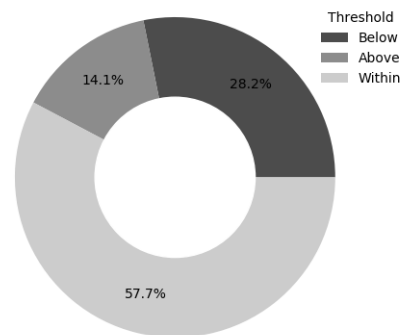
(a) Lambrate



(b) P.zza Zavattari

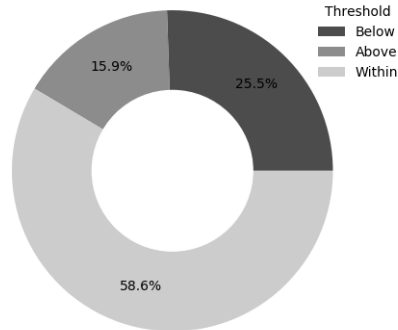


(c) V. Brera



(d) V. Marche

BE SECURE



(e) V. Juvara

Figure 6: Hourly averaged temperature frequency distribution according to the threshold limits set (i.e. 9-26 °C) for every selected weather station.

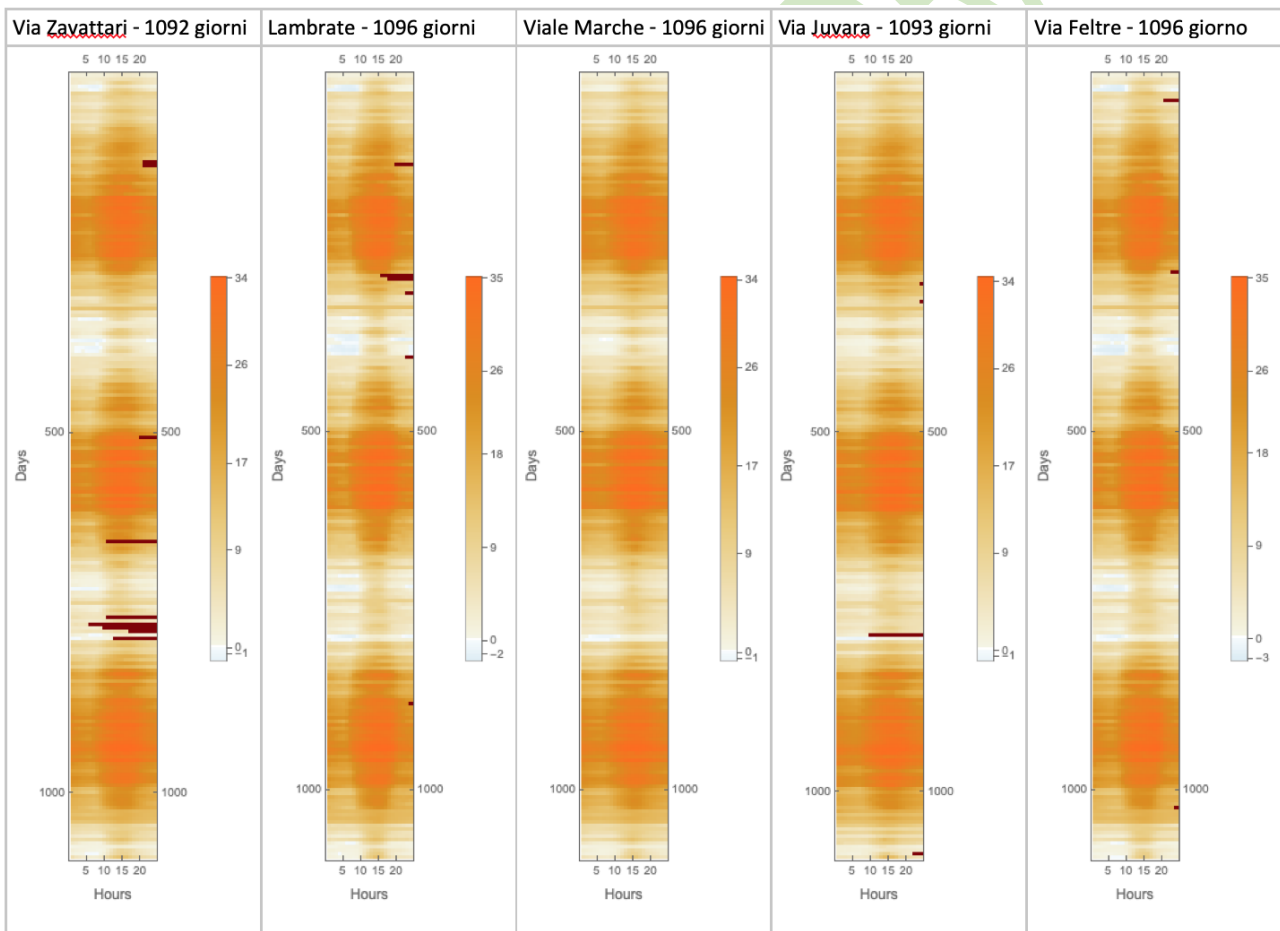


Figure 7: Hourly average temperature from 2016 to 2018 for the weather stations.



b. Precipitation and relative humidity

Figure 8 and Figure 9 present the historical data on precipitation recorded by the selected weather stations from 2017 to 2019. The charts show that the winter season is in general the period of the year when the precipitations are frequent, but the quantity of water read is less abundant. This is confirmed both by the hourly average data (Figure 8) and by the daily average historic data (Figure 9), showing large peaks of mm of rain far from January.

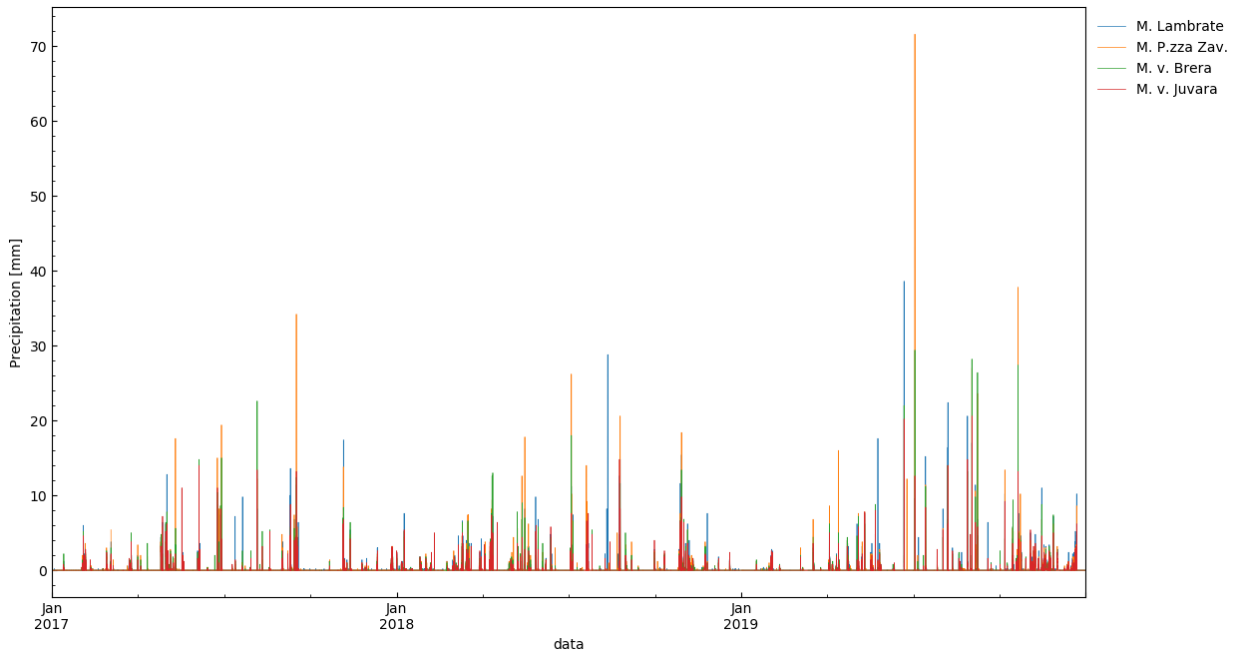


Figure 8: Hourly average of precipitation readings for selected weather stations.

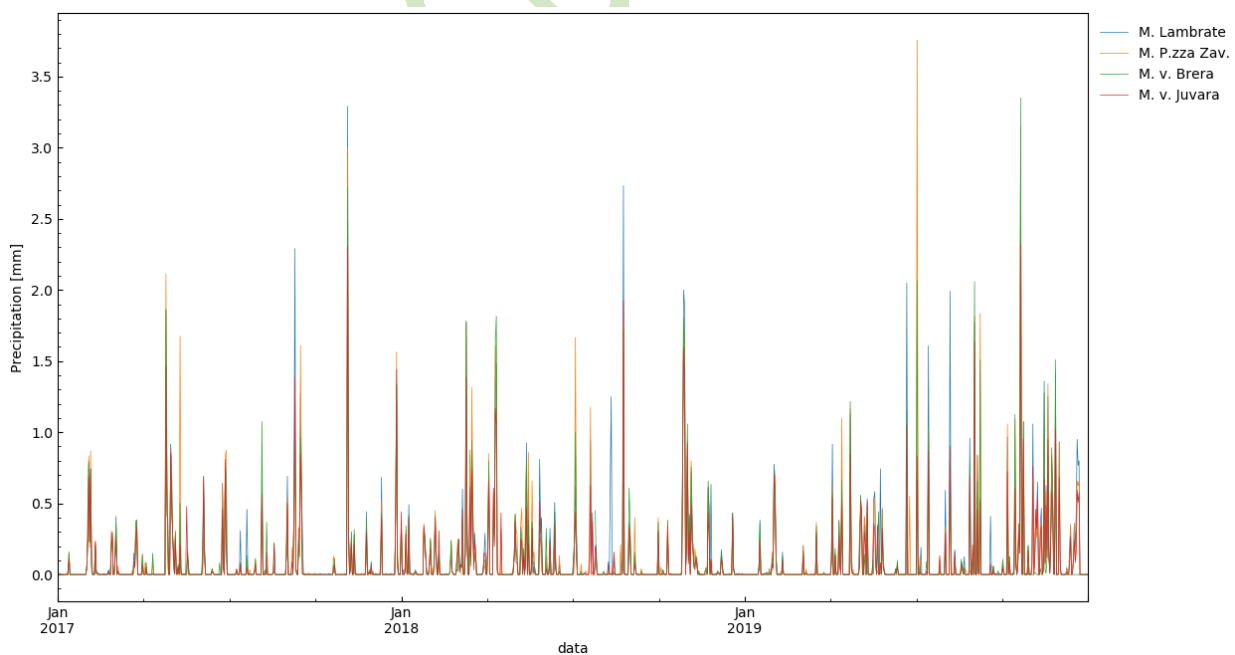


Figure 9: Daily average of precipitation readings for selected weather stations.

Nevertheless, the district data of the Relative Humidity (RH) registered for the considered weather centrals, show a counter tendency compared to the precipitation historic data. The RH values increase during the winter season, due to the effects of decreasing temperatures (frequent rain and less water vapor carrying capacity). This trend is confirmed by the trend displayed in Figure 10 and Figure 11 representing respectively the RH hourly and daily average.

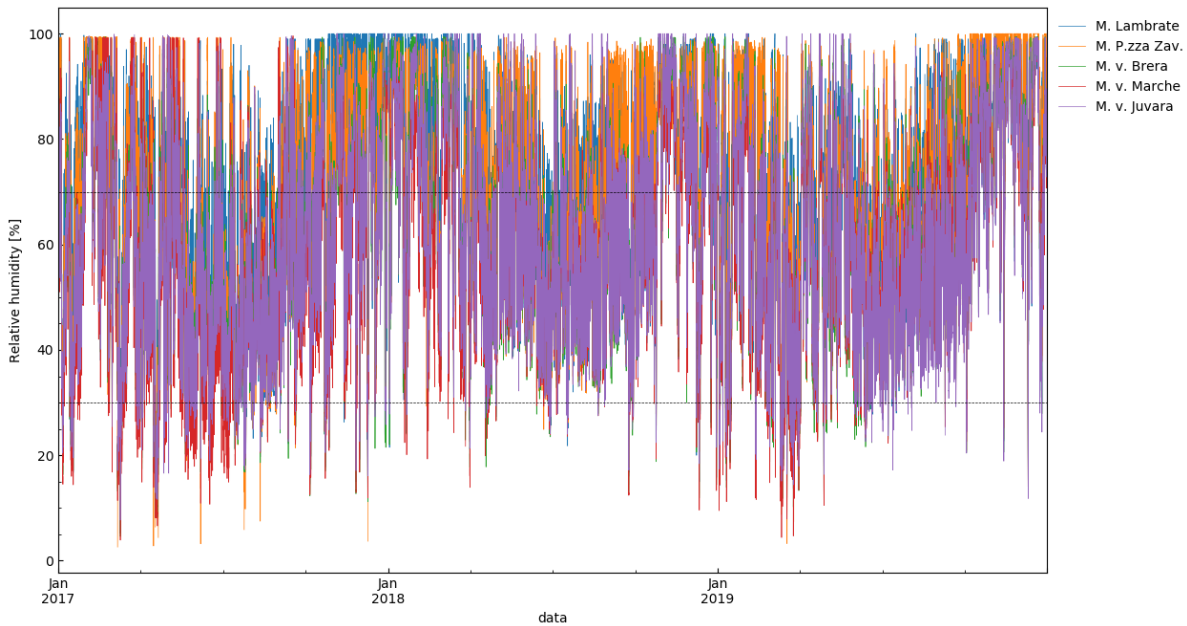


Figure 10: Hourly average of relative humidity readings for selected weather stations. Dotted lines demark lower and upper thresholds for humid and dry stettings (according to indoor comfort deifnition (EN-ISO-7730 2005)).

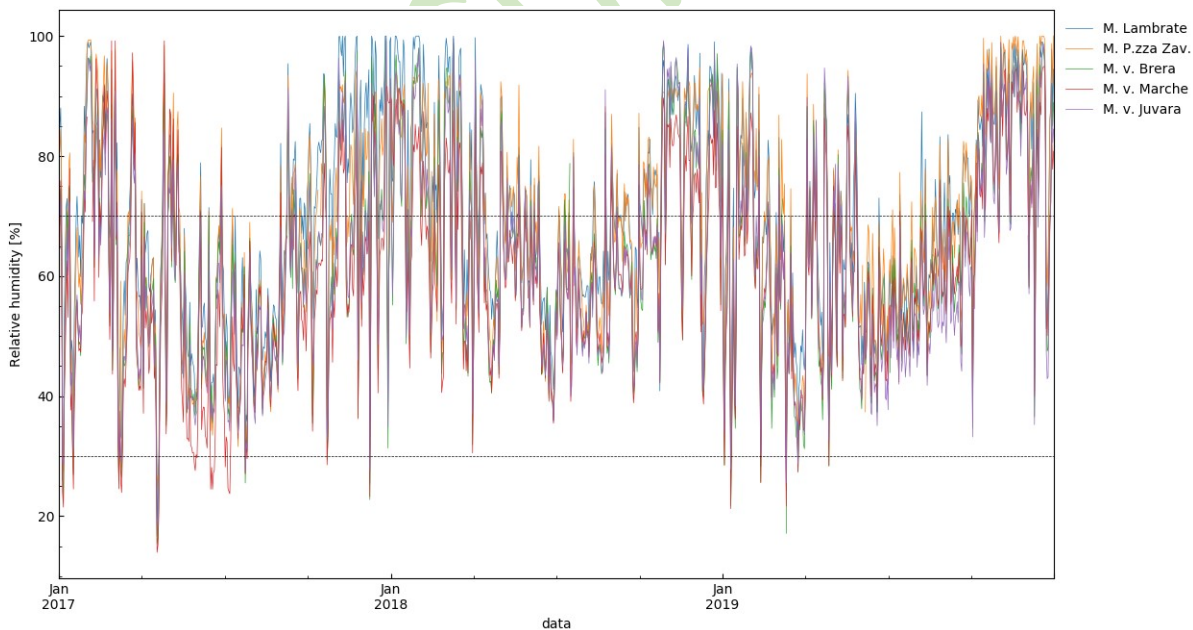
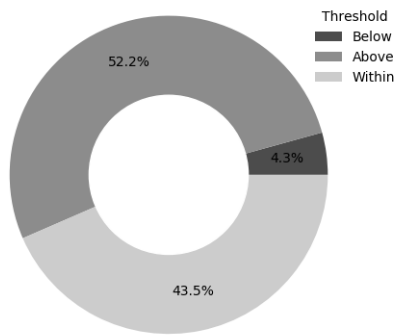
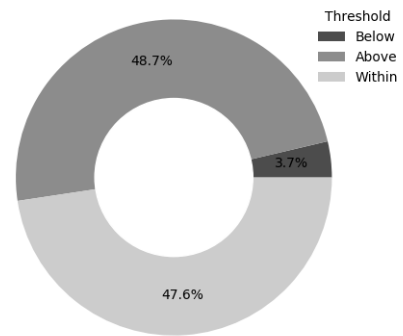


Figure 11: Daily average of relative humidity readings for selected weather stations. Dotted lines demark lower and upper thresholds for humid and dry stettings (according to indoor comfort deifnition (EN-ISO-7730 2005)).

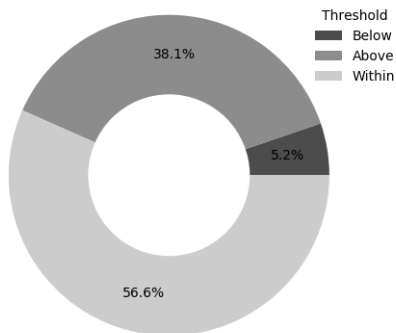
Figure 12 shows that 3 out of the 5 considered weather stations reported more frequently values within the comfort thresholds, Lambrate and Piazza Zavattari stations recorded instead rather humid conditions (i.e. RH above 70%).



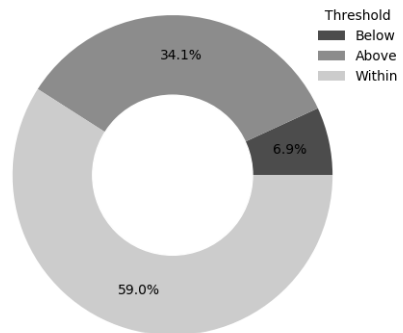
(a) Lambrate



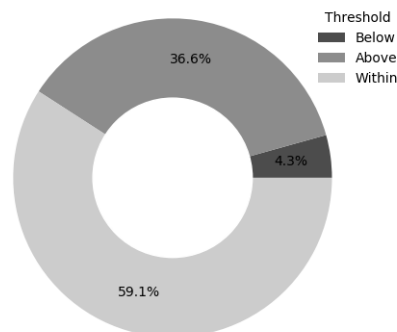
(b) P.zza Zavattari



(c) V. Brera



(d) V. Marche



(e) V. Juvara

Figure 12: Hourly averaged relative humidity frequency distribution according to the threshold limits set (i.e. 30-70 %) for every selected weather station.

These stations are located in two different urban areas: rather peripheral for Lambrate and more central for Piazza Zavattari. Not revealing at a glance, a possible correlation between the location of the sensors and the HR frequency values. A more detailed comparison can be done when considering the built environment characteristics surrounding the station.

c. Wind velocity

Figure 13, Figure 14, Figure 15 represent historic data on wind velocity from 2016 to 2019. Figure 14, Figure 15 represent also the comfort threshold for inhabitants. Observing these representations, it is clear that the wind velocity increases during spring and summer months, while decreasing during winter. This trend could also be responsible for higher levels of air pollutants' concentration during winter, as introduced in §Errore. **L'origine riferimento non è stata trovata.** and extensively described in the D2.2.2.

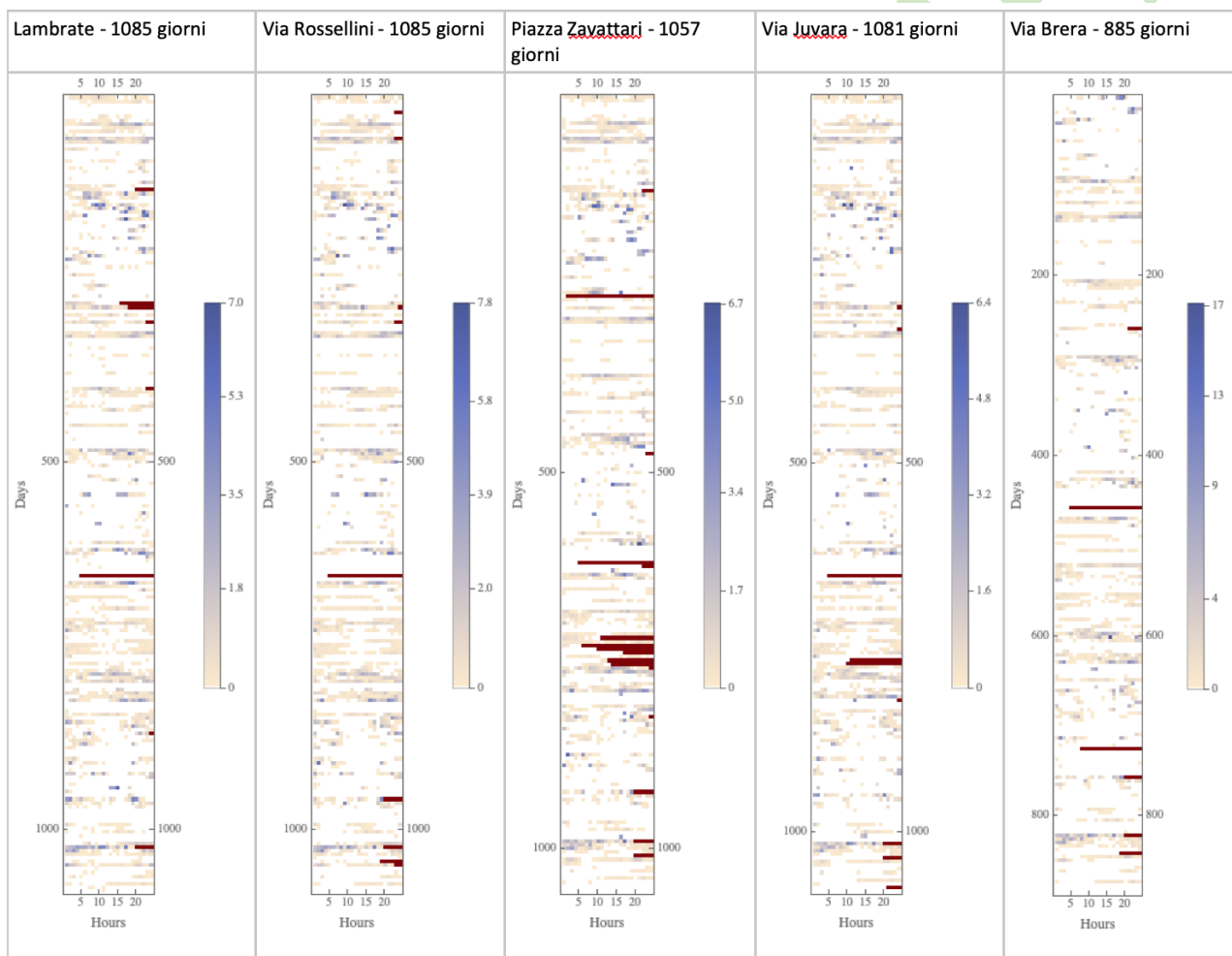


Figure 13: Hourly average rainfall mm from 2016 to 2018 for the weather stations.



BE SECURE

(make) Built Environment Safer in Slow and Emergency Conditions through behaviorally assessed/designed Resilient solutions

Grant number: 2017LR75XK

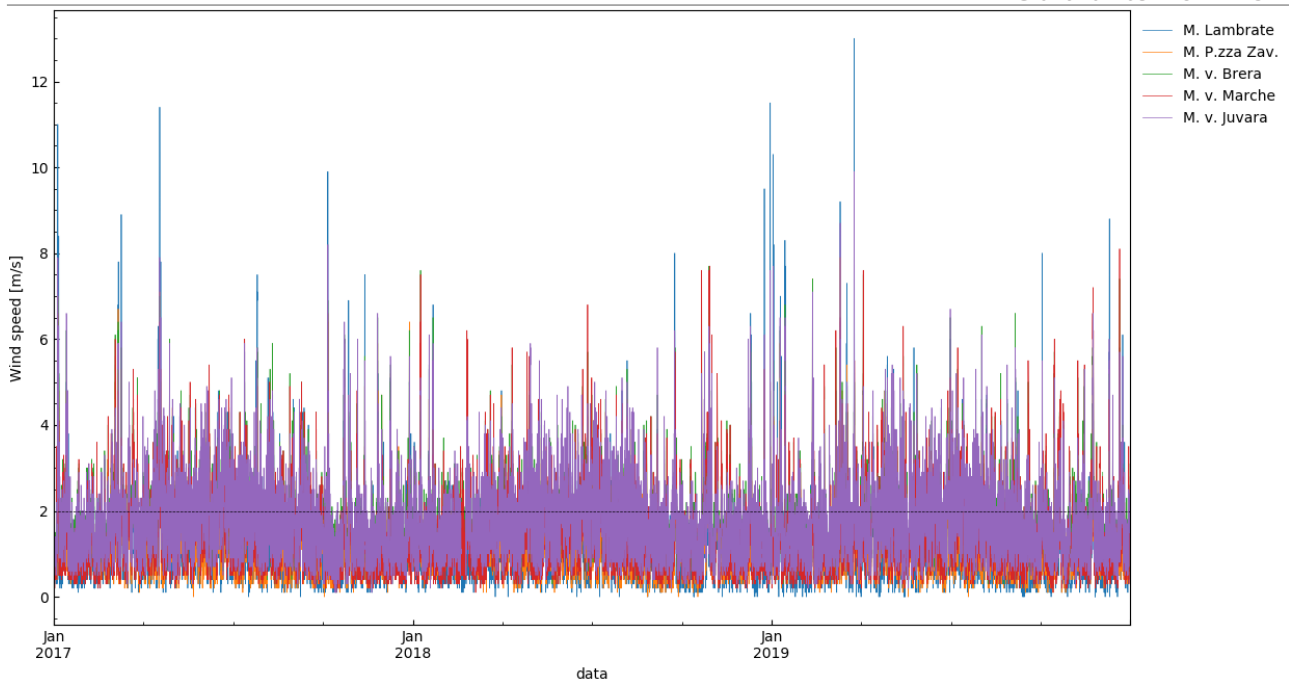


Figure 14: Hourly average wind velocity readings for selected weather stations. Dotted lines demark the 2 m/s thresholds which mainly accounts for low ventilated spaces; according to indoor conditions review (EN-ISO-7730 2005).

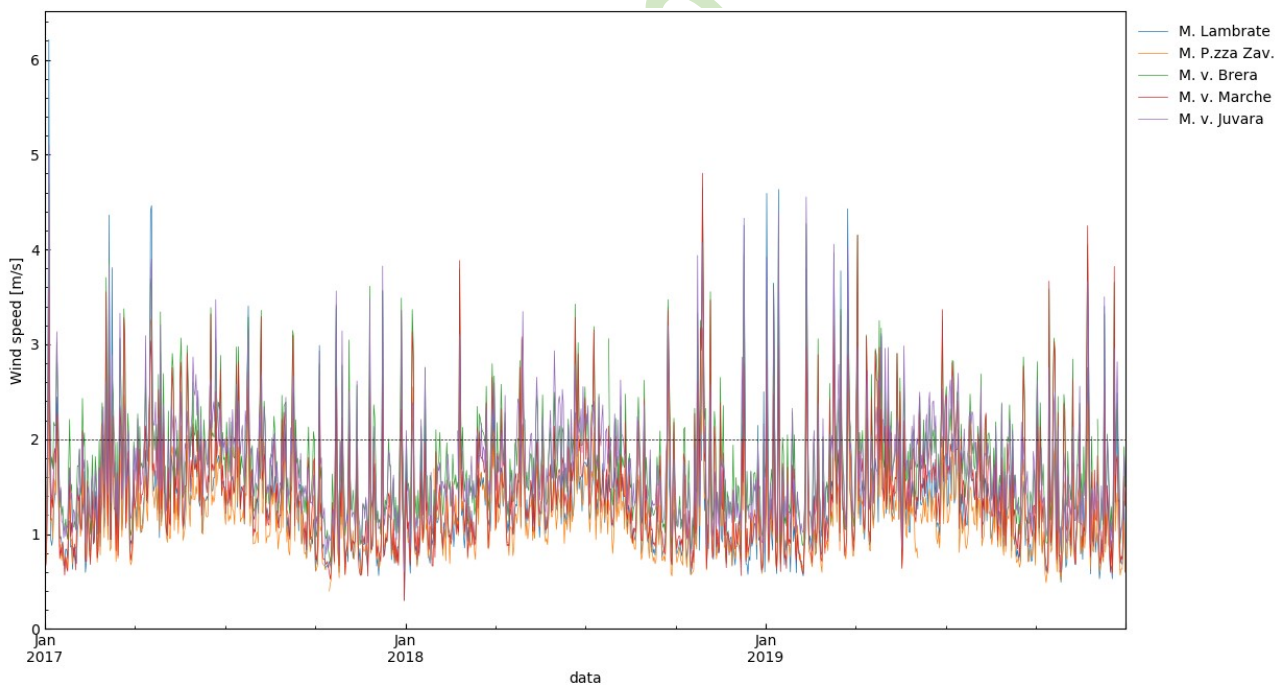
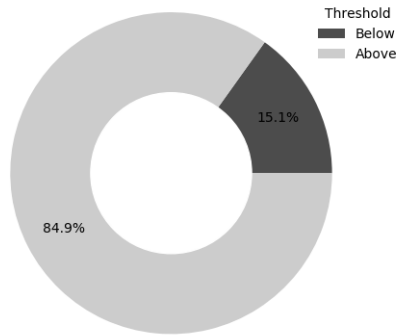
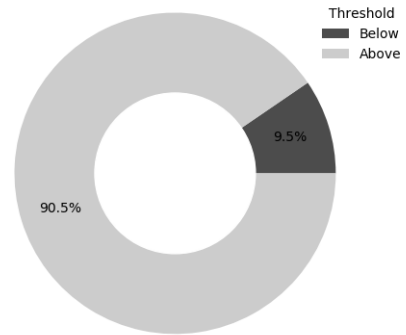


Figure 15: Daily average of wind velocity readings for selected weather stations. Dotted lines demark the 2 m/s thresholds which mainly accounts for low ventilated spaces; according to indoor conditions review (EN-ISO-7730 2005).

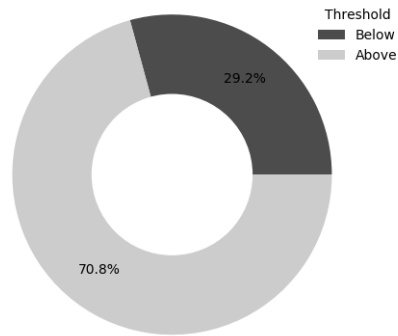
However, these values seldom exceed the comfort threshold as represented in Figure 16. Among the 5 selected weather stations, *v. Brera* and *v. Juvara* are reporting more values below the threshold for the 2017-2019 period. These could be related to the fact that they are closer to the city's downtown (denser areas).



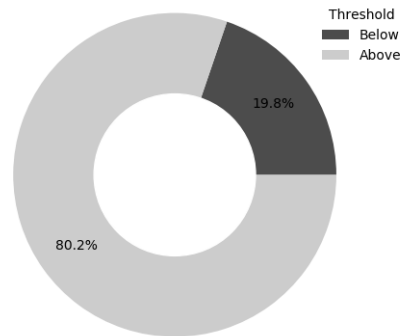
(a) Lambrate



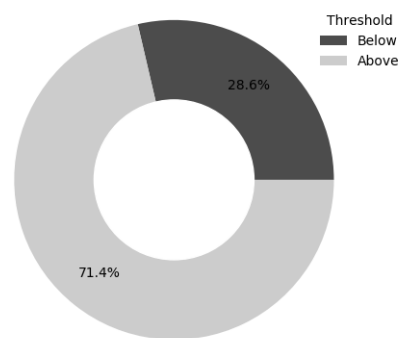
(b) P.zza Zavattari



(c) V. Brera



(d) V. Marche



(e) V. Juvara

Figure 16: Hourly averaged wind velocity frequency distribution according to the threshold limit set as useful (i.e. 2 m/s) for every selected weather station.

The fact that the station reporting the least frequent values above the threshold is higher than the 70% of the time is optimistic to reduce the potential risk at high air temperatures.

d. Global horizontal radiation

For the solar radiation, the same types of analyses already described for the previous historic data have been accomplished for the period 2017-2019. However, in this case, a set of three stations' sensors have been considered: those of *Lambrate*, *via Brera* and *Viale Juvara* (Figure 17, Figure 18, Figure 19).

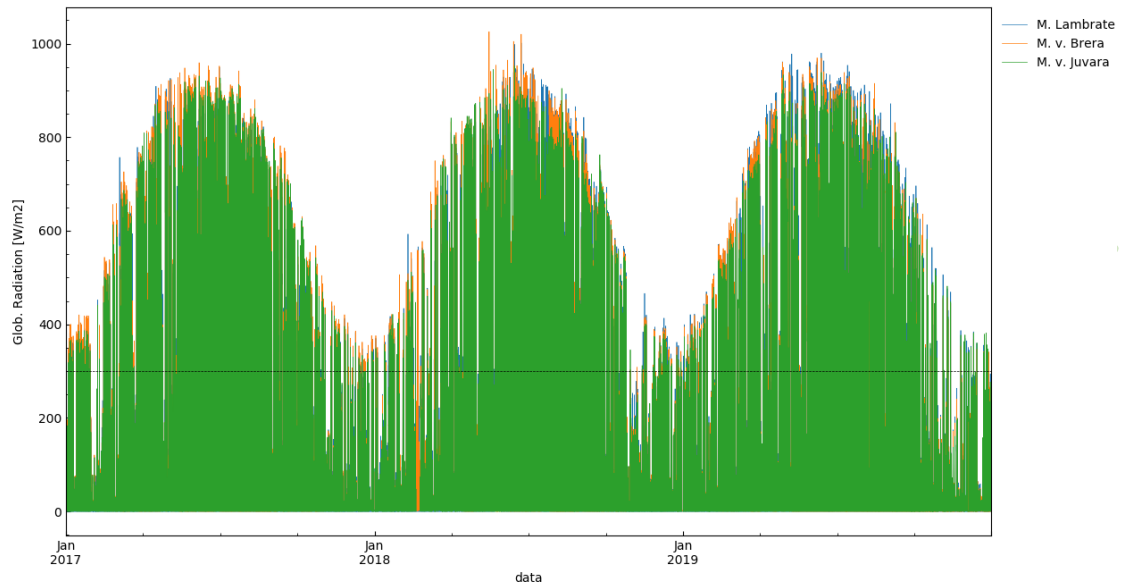


Figure 17: Hourly average of global horizontal radiation readings for selected weather stations with available data. Dotted lines demark 300 W/m² threshold, which represents a significant warmer temperature perception when stricken (Lyons et al. 2000; Cheng and Ng 2006).

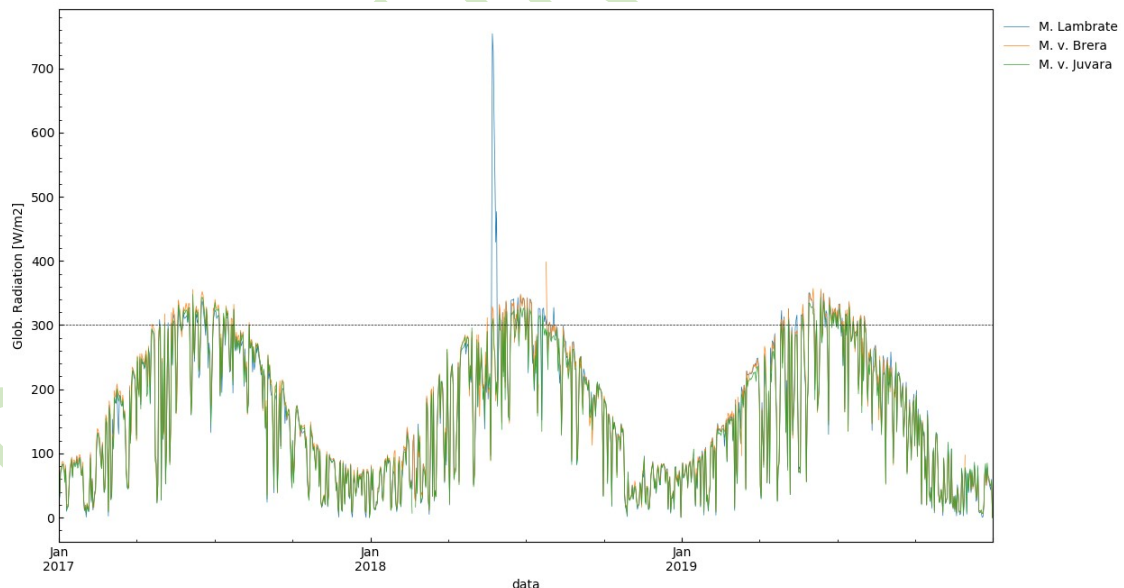


Figure 18: Daily average of global horizontal radiation readings for selected weather stations with available data. Dotted lines demark 300 W/m² threshold, which represents a significant warmer temperature perception when stricken (Lyons et al. 2000; Cheng and Ng 2006).

Also, in this case, the intensity trend follows the seasons, increasing during spring and reaching the peak values in summer; then decreasing in autumn and reaching the minimum values in winter. Values recorded

by the three sensors are very similar during all the considered period (2017-2019) except for the Lambrate sensor, registering during summer 2018 a very high value. This is probably an outlier value, due to a sensor failure.

Figure 19 represents the frequencies of registered values above and below the comfort threshold. The threshold of 300 W/m^2 is never exceeded more than one-quarter of times in the considered period.

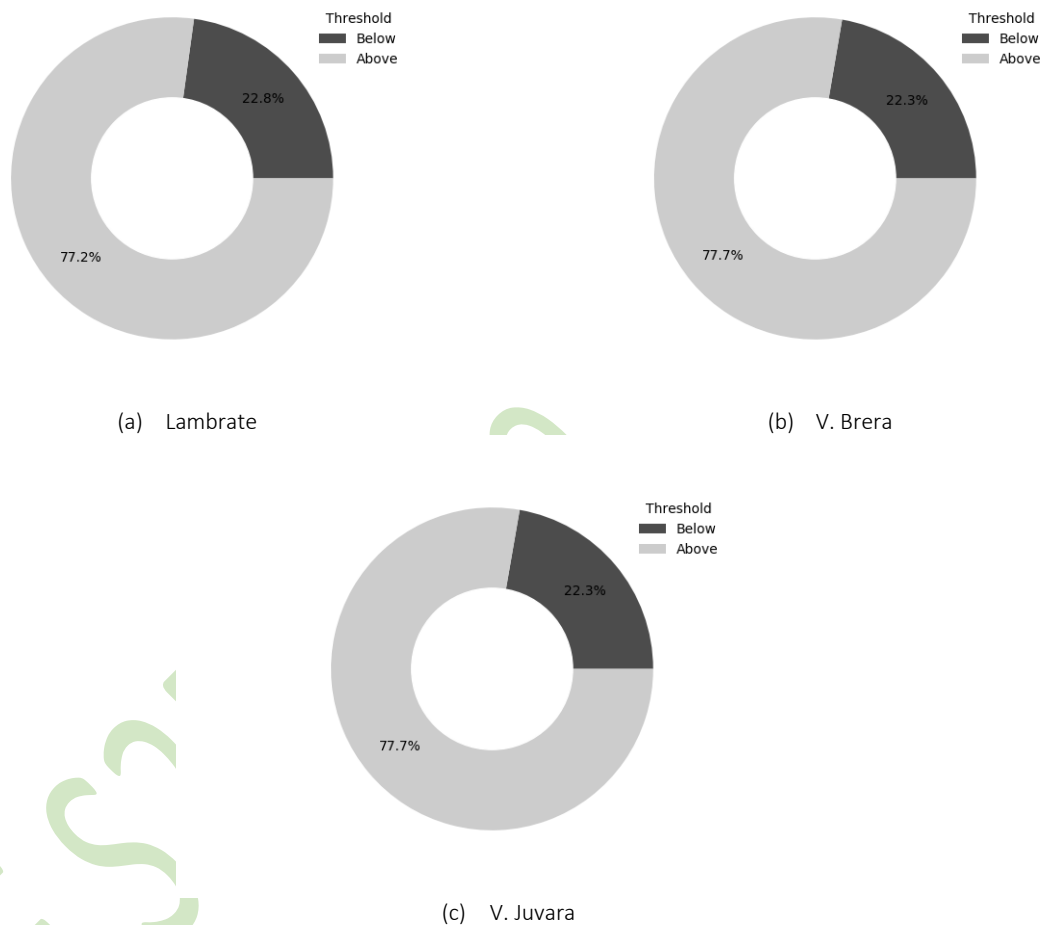


Figure 19: Hourly averaged horizontal global solar radiation frequency distribution according to the threshold limit set as significant for temperature perception increase (i.e. 300 W/m^2) for every selected weather station. P.zza Zavattari and V. Marche have been excluded as they do not have the sensor for monitoring this parameter.

The hourly average radiation has been also represented in Figure 20, allowing a comparison among the three active sensors. Dark red bars represent missing values for the specific day. The data of some sensors seems to be not very reliable. Moreover, 2019 data for all the three sensors are completely unreliable, therefore they have not been considered.



BE SECURE

(make) Built Environment Safer in Slow and Emergency Conditions through behavioral assessed/designed Resilient solutions

Grant number: 2017LR75XK

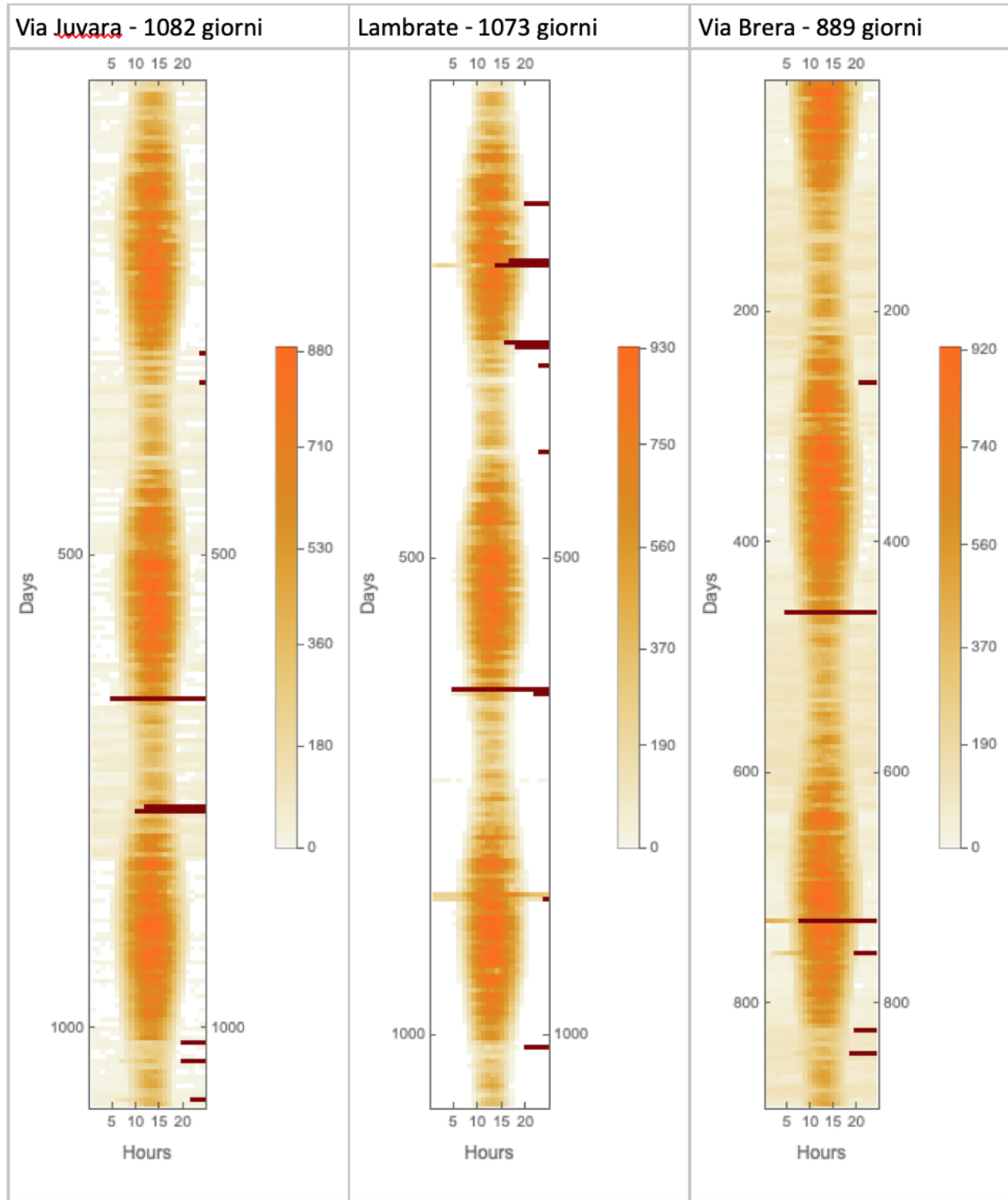


Figure 20: Hourly average radiation from 2016 to 2018 for the weather stations.

e. Variations related to the built environment

Analyses in terms of the presence of green areas and density of the BE, presented in previous reports, allow making some insights on the data detected by the considered weather sensors. A summary of the frequency of readings of disadvantageous conditions for each weather station has been presented in Table 2. That is, temperatures and radiation above the threshold, relative humidity outside the comfort range, and wind speed below the threshold.

For instance, recalling the results for the weather stations of *Lambrate*, *P.zza Zavattari* and *v. Marche* reporting low frequency of air temperatures above the threshold they are all either in an area of high green area coverage (i.e. *Lambrate*, see Figure 1 and Figure 21) or close to a rather low-density space which might have features that not favor heat entrapment (i.e., *P.zza Zavattari* and *v. Marche*, see Figure 1 and Figure 22). On the other hand, *v. Brera* reported a lower frequency of high temperatures as well, while immersed in a dense area, this could be achieved perhaps by geometrical properties that favor wind flow as the frequency of hours above 2 m/s is the highest.

The case of *v. Juvara* is rather interesting, given that when analyzing Figure 1, Figure 21 and Figure 22 it is an area of low green area coverage and high density, and still has the most recurrent air temperature above threshold condition. This occurs even when the wind velocity is considerably frequent above 2 m/s (i.e. 28.6 % of the time). Therefore, it has been assumed that there are particular features of the built environment that have restricted the heat management process.

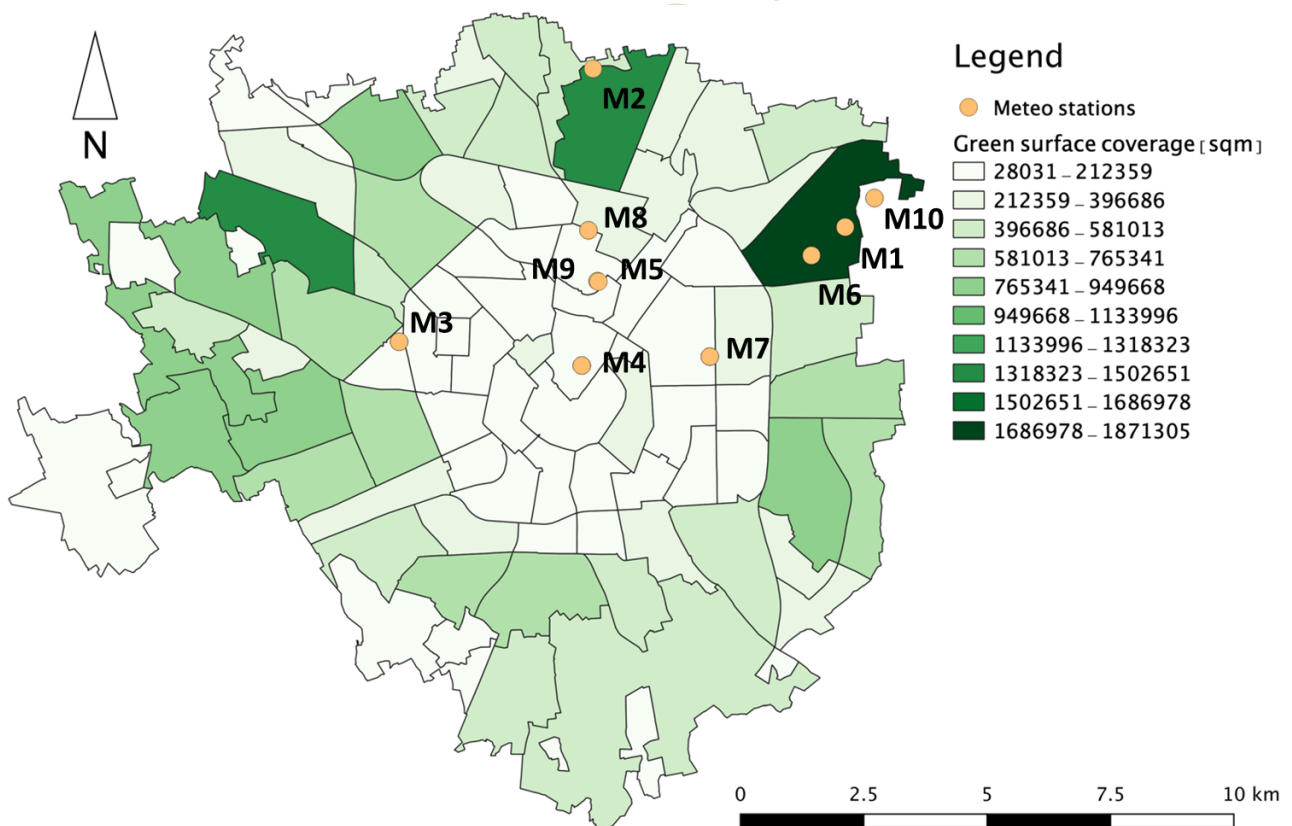


Figure 21: Total green areas coverage per Local Identity Unit (NIL from the acronym in Italian) (extracted and edited from D.2.1.2).

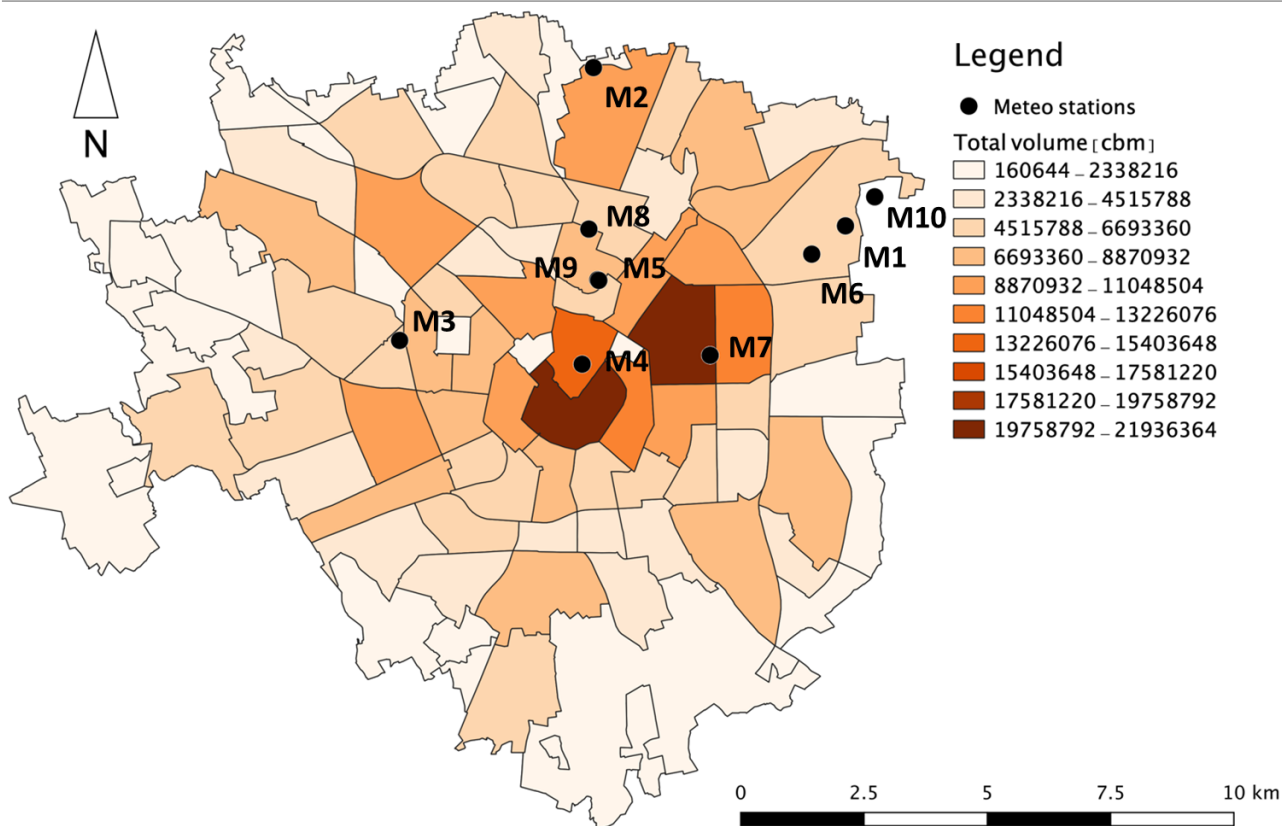


Figure 22: Total built volume in the Local Identity Unit (extracted and edited from D.2.1.2).

Station	BE condition		Disadvantageous frequency [%]			
	Green coverage	Density	Air temperature	Relative humidity	Wind velocity	Radiation
M. Lambrate	Very High	Avg. / low	14.1	56.5	15.1	77.2
M. P.zza Zavattari	Low	Low	14.3	52.4	9.5	
M. v. Marche	Low	Avg. / low	14.1	41.0	19.8	
M. v. Juvara	Low	Very High	15.9	40.9	28.6	77.7
M. v. Brera	Low	High	14.2	43.3	29.2	77.7

Table 2: Summary of the conditions of the screened weather stations around the city of Milan.

2. Implications on the selected area in Città Studi

The station of *Milano v. Juvara* is the closest to the case study area (in the Città Studi neighborhood) described in D2.1.1. This neighborhood is characterized by low green area coverage and very high BE density. In addition, the *Milano v. Juvara* station reports the worst condition for air temperature above 26°C (i.e. 15.9% of hours during the period of 2017-2019), combined with the second-highest frequency of disadvantageous wind velocity conditions (i.e. 28.6% of hours during the period of 2017-2019).

These characteristics play an important role to highlight the significance of the delineated city region. However, these values might be biased or skewed depending on the location of the weather station. In fact, solar radiation is measured unobstructed, wind speed normally is measured at 10 m height, nearby water bodies might modify the air humidity content and temperature.

In this particular location, further studies were performed, determining the distribution frequency of values in the previous 3 years (to provide an overview of the probability of occurrence). This allows to scale down the analyses to the area we are assessing, thus, to start analyzing in depth what is going on and what the subsequent measurements would do.

2.1 Distribution frequency function

This analysis allows to investigate how the temperature values are distributed in temperature range bins along the period of analysis. Also, it can be split into seasons so to have a much-fit function, enabling higher detail as *increasing temperatures* SLOD is clearly more frequent during summer (Figure 4 and Figure 5) and, depending on the pollutant, the *air pollution* SLOD can be critical in both seasons; but, the weather conditions will represent a relief or a stressor for the SLOD itself.

a. Air temperature

The analyses show in Figure 23, Figure 24 and Figure 25 represent the frequencies of the values detected by the *v. Juvara* weather station in the period 2016-2019. Figure 23 represent the whole historic dataset, revealing mainly three peaks corresponding to the winter, summer seasons and to spring and autumn seasons when the temperatures are comparable

In order to better represent the data, the same analysis has been accomplished selecting only data related to the winter (Figure 24) and summer (Figure 25) season in the period 2016-2019. This revealed a peak for the winter season between 5-10°C and a minor one around 15°C. For the summer season, the most frequent detected temperature is around 25°C and the average is 22.5°C. These values, despite being within the comfort thresholds 9°-26°C, they are next to the discomfort condition as represented in Figure 3.

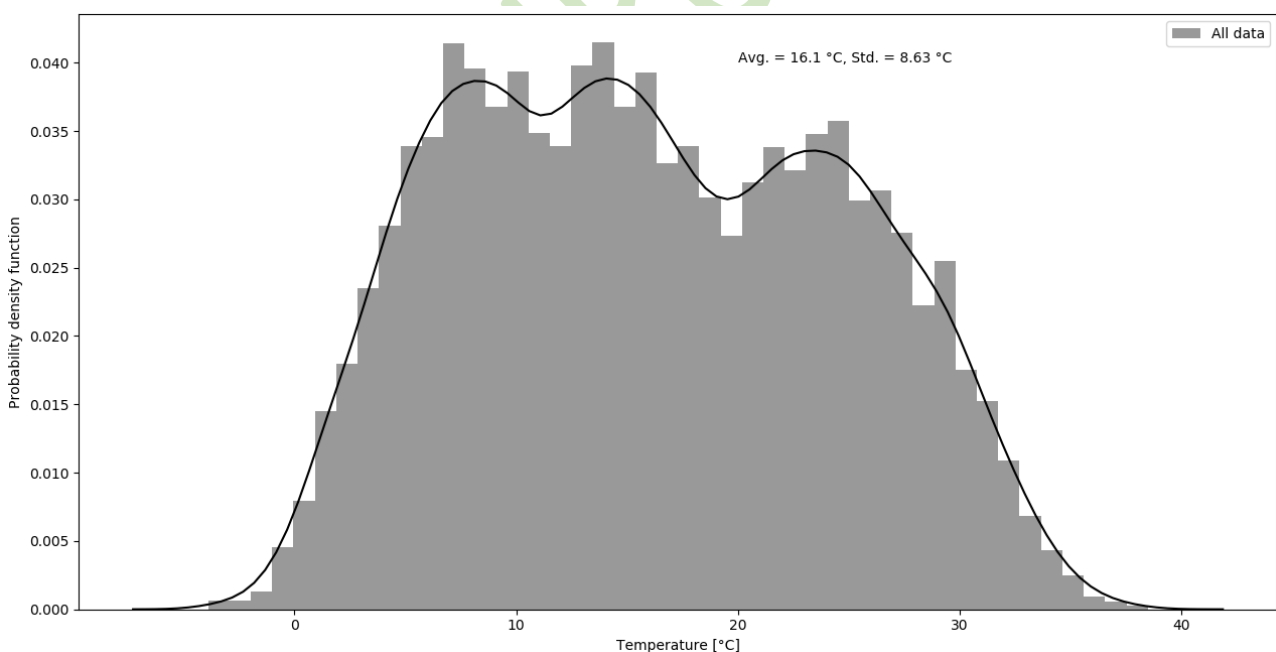


Figure 23: Temperature probability distribution function of air temperature values from 2016 to 2019. Highlighting value average and standard deviation.



BE S²ECURE

(make) Built Environment Safer in Slow and Emergency Conditions through behavioral assessed/designed Resilient solutions

Grant number: 2017LR75XK

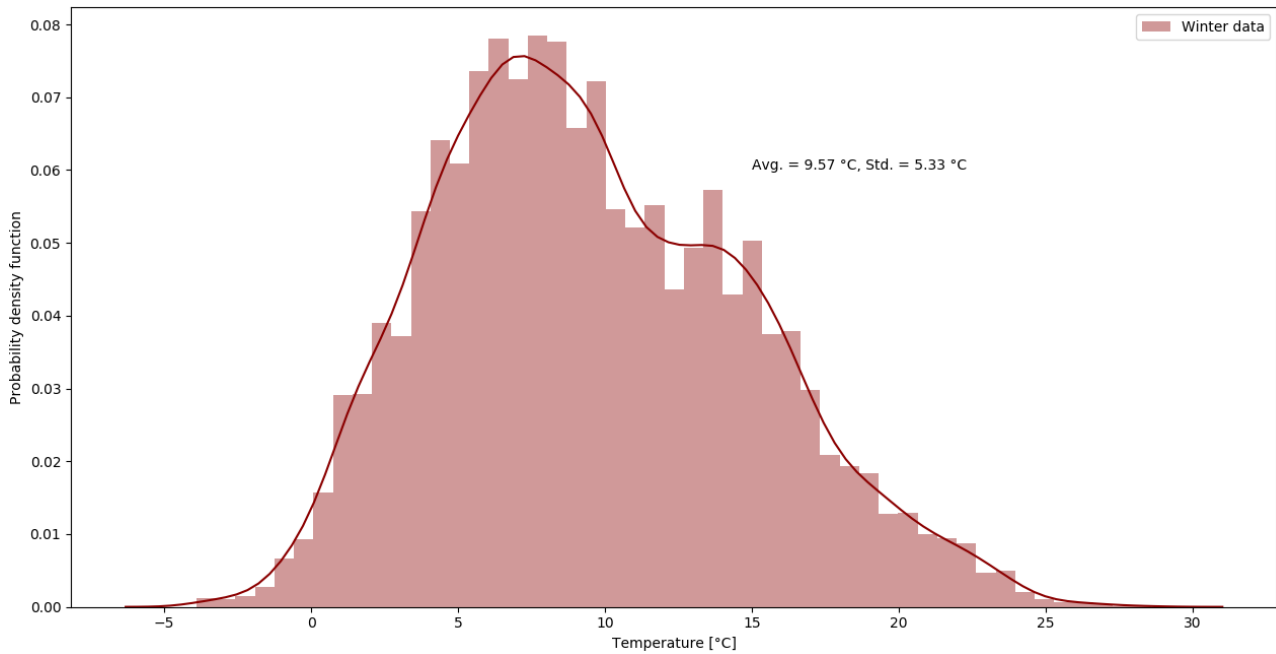


Figure 24: Temperature probability distribution function of air temperature values from the winter season from 2016 to 2019. Highlighting value average and standard deviation.

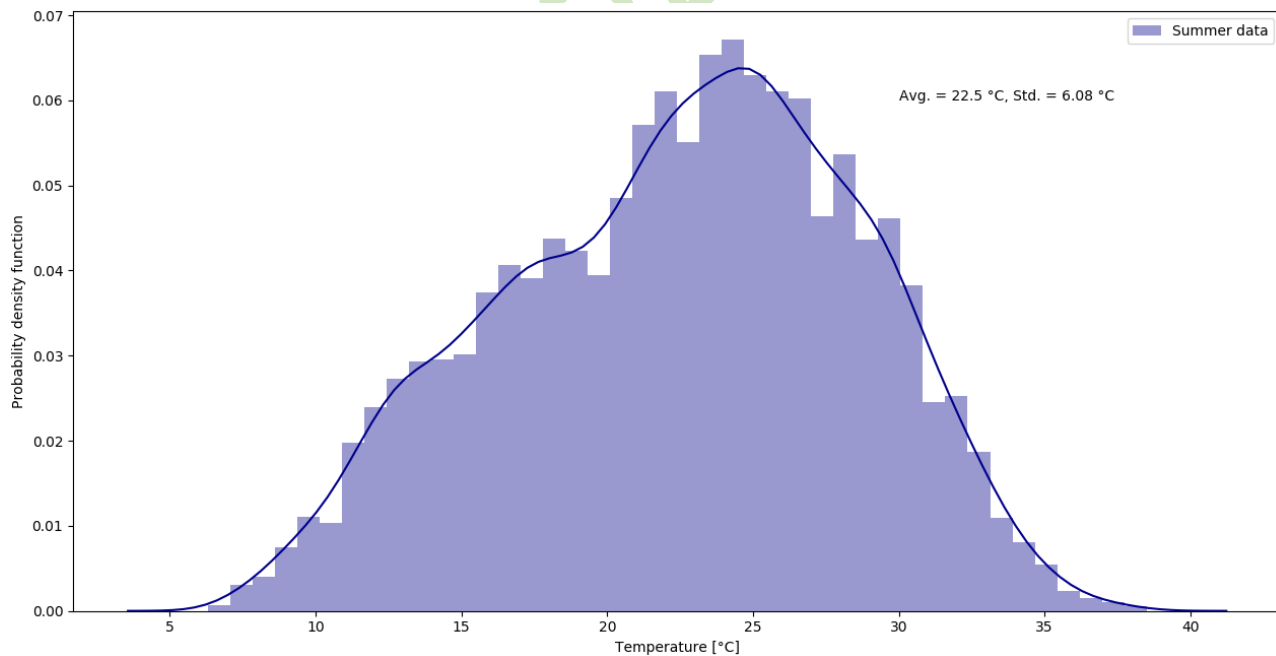


Figure 25: Temperature probability distribution function of air temperature values from the summer season from 2016 to 2019. Highlighting value average and standard deviation.

b. Relative humidity

The same type of analyses have been accomplished for the RH detected for the period 2016-2019 by the v. Juvara weather station.

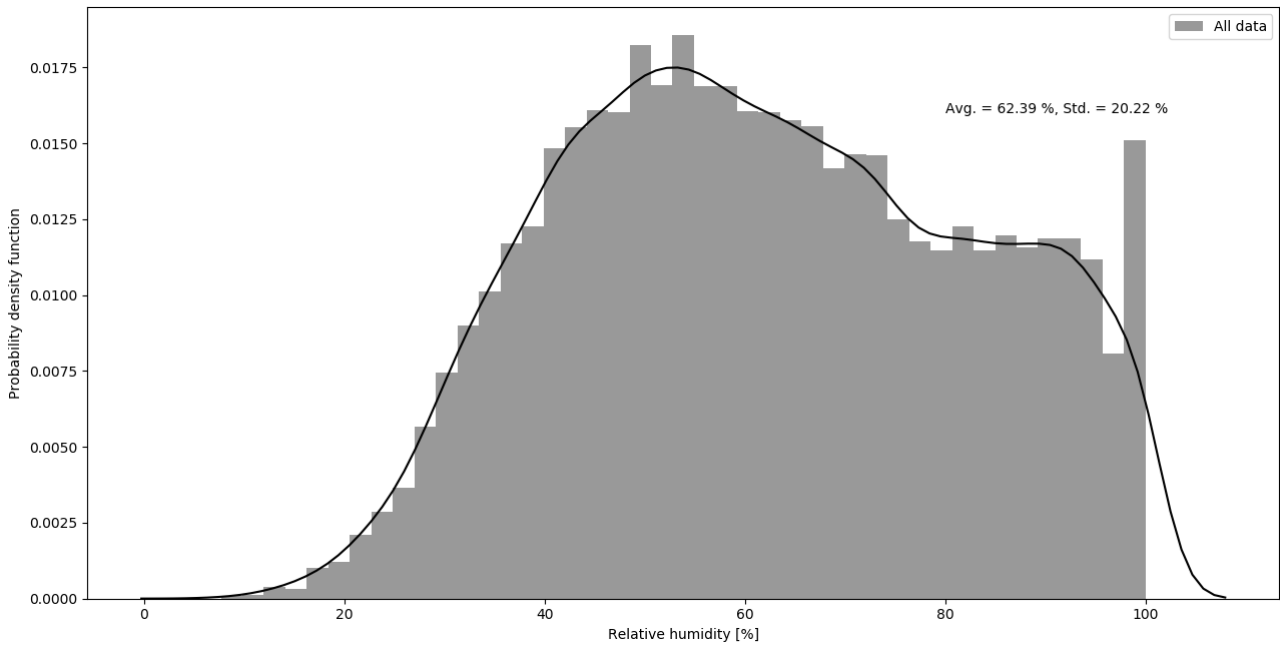


Figure 26: Relative humidity probability distribution function for values from 2016 to 2019. Highlighting value average and standard deviation.

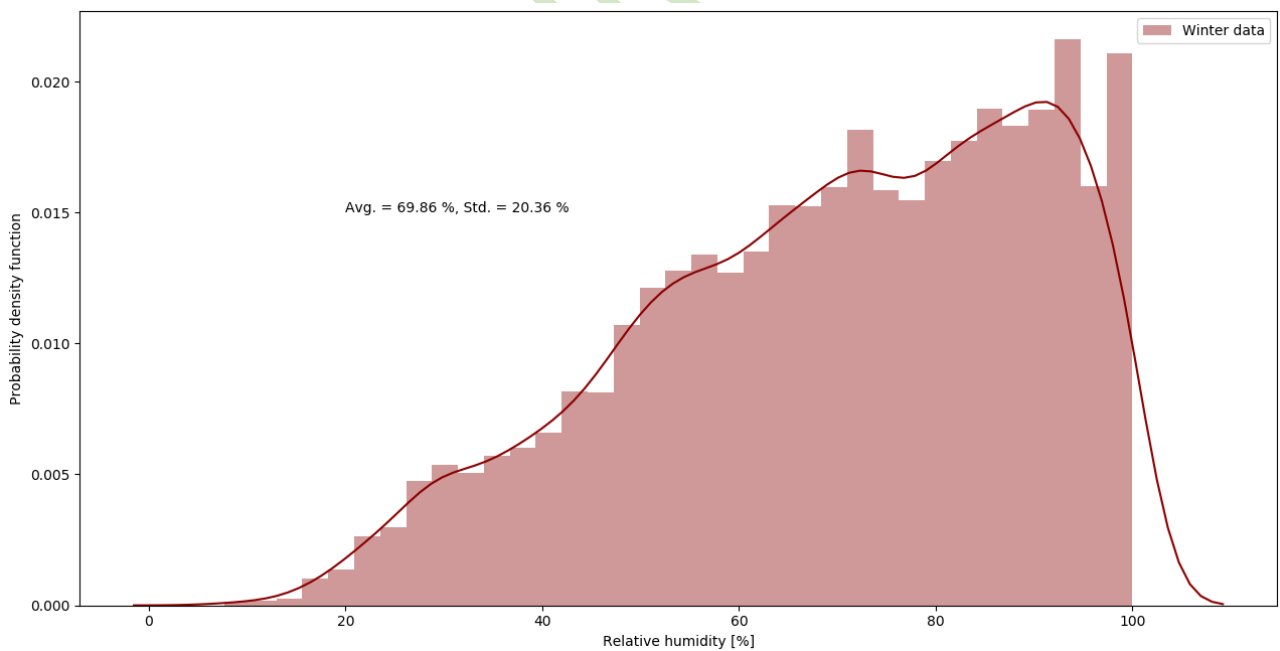


Figure 27: Relative humidity probability distribution function for winter season values from 2016 to 2019. Highlighting value average and standard deviation.

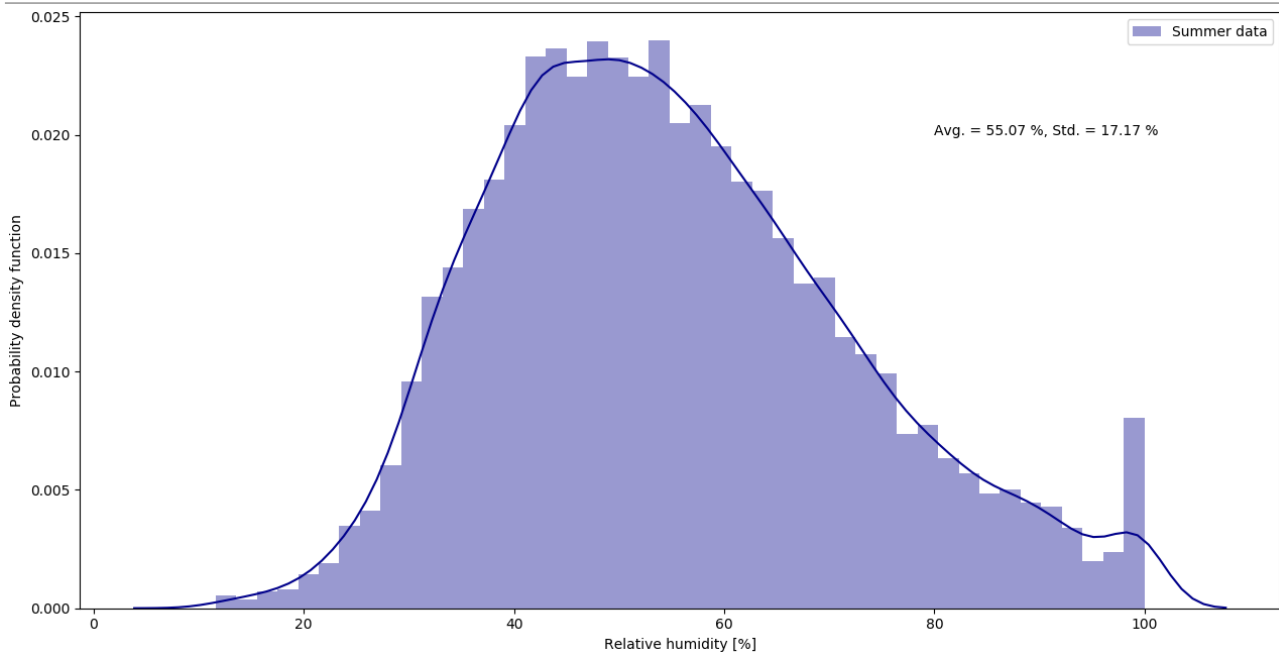


Figure 28: Relative humidity probability distribution function for summer season values from 2016 to 2019. Highlighting value average and standard deviation.

The results of the comprehensive analysis on the whole dataset is represented in Figure 26, while the insights for the winter (Figure 27) and summer (Figure 28) seasons have been carried out on a subset of the whole available data. These analyses demonstrate that the average value during winter is at the upper threshold of the indoor comfort condition (30-70%), despite this is an average value. The peak of the PDF is around HR=90%.

It must be noted that also for winter the conditions are not ideal, having an average of ~55% and a standard deviation of ~17% (Figure 28), which means that by a considerable time, the area is having a rather humid air. This might be worsening the temperature perception of the people in the zone. Summer might be characterized as rather warm and humid.

c. Wind velocity

The same analyses carried out for the wind velocity show higher values in the summer season and similar PDF for values registered by the sensor, calculated for the whole dataset and only for the winter values Figure 29 and Figure 30. However, the PDF for the summer season has a different shape and therefore, presents a different distribution of the detected values. In summer the average value is closer to the comfort threshold of 2m/s.

Meaning that the wind might help alleviate the previously mentioned conditions of warm and humid by introducing a rather frequent breeze.



BE S²ECURE

(make) Built Environment Safer in Slow and Emergency Conditions through behaviorally assessed/designed Resilient solutions

Grant number: 2017LR75XK

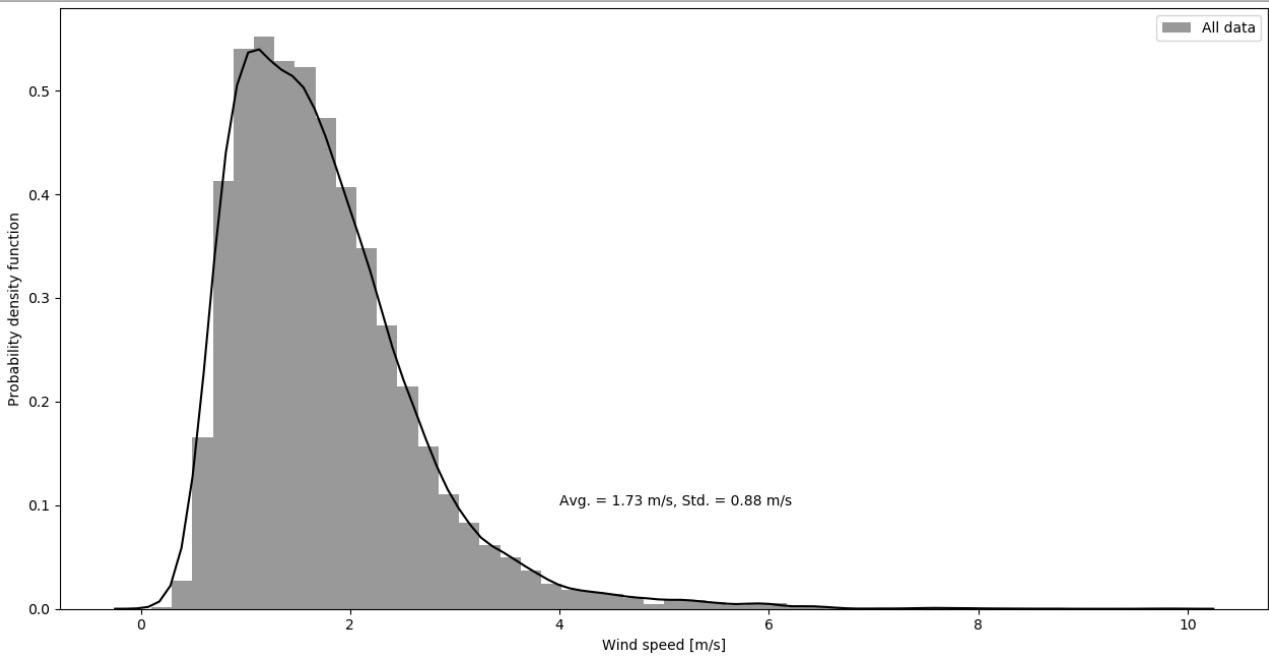


Figure 29: Wind speed probability distribution function for values from 2016 to 2019. Highlighting value average and standard deviation.

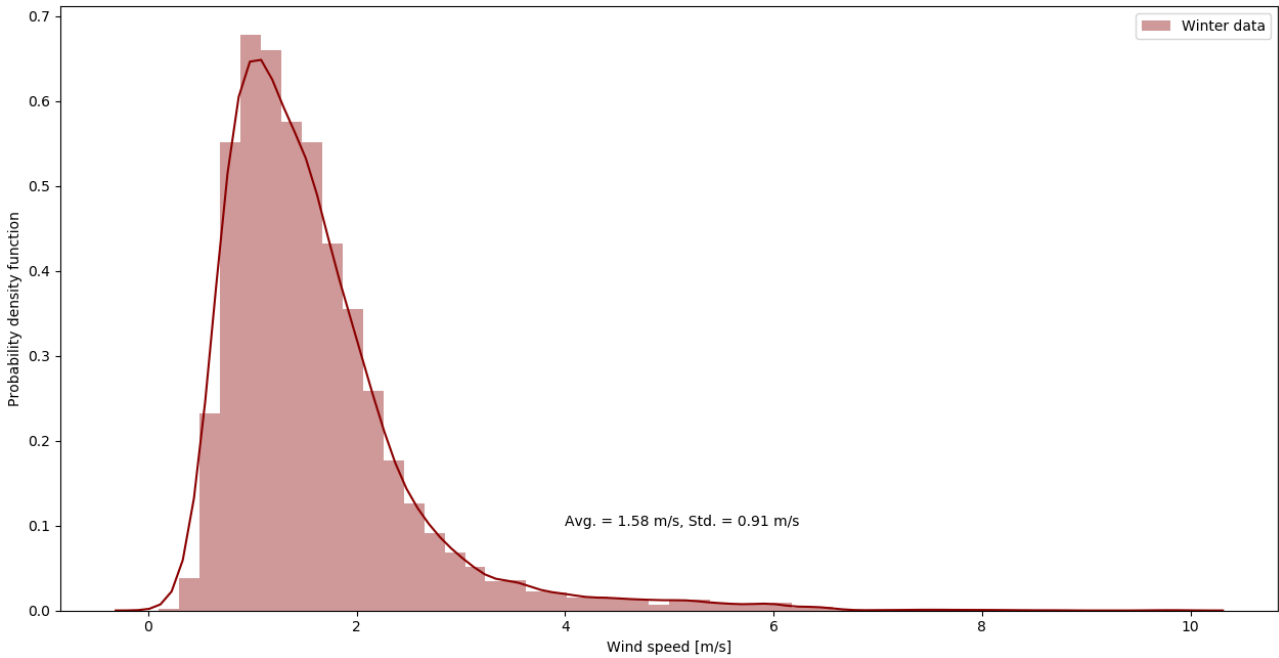


Figure 30: Wind speed probability distribution function for winter season values from 2016 to 2019. Highlighting value average and standard deviation.

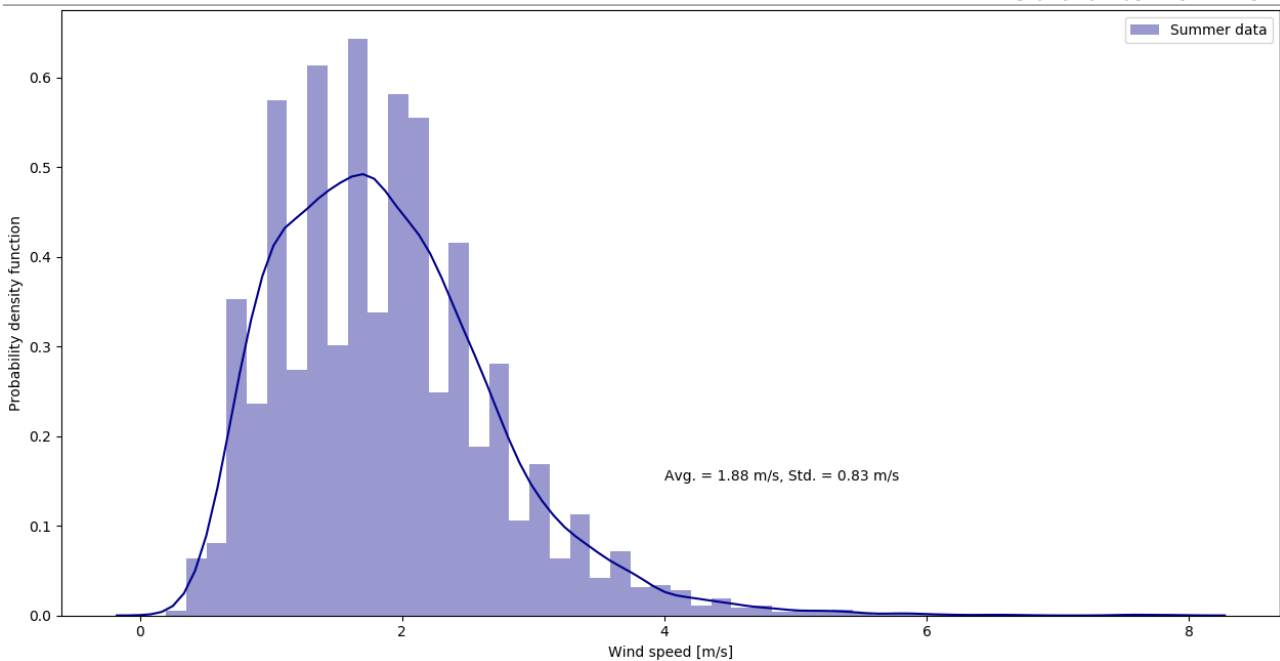


Figure 31: Wind speed probability distribution function for summer season values from 2016 to 2019. Highlighting value average and standard deviation.

d. Incident radiation

PDFs for the horizontal global solar radiation calculated for the whole dataset and the selected winter and summer data varies remarkably (Figure 32, Figure 33 and Figure 34). However, average values or the three charts are never above the comfort threshold 300 W/m^2 .

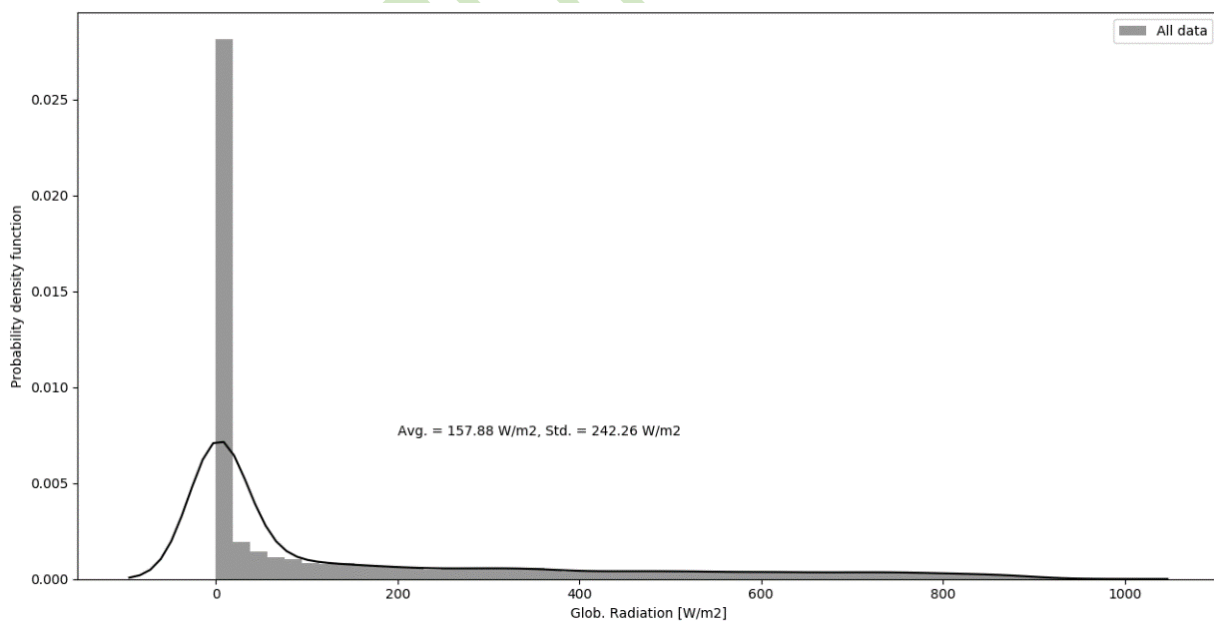


Figure 32: Probability distribution function of the Horizontal global solar radiation, considering values from 2016 to 2019. Highlighting value average and standard deviation.

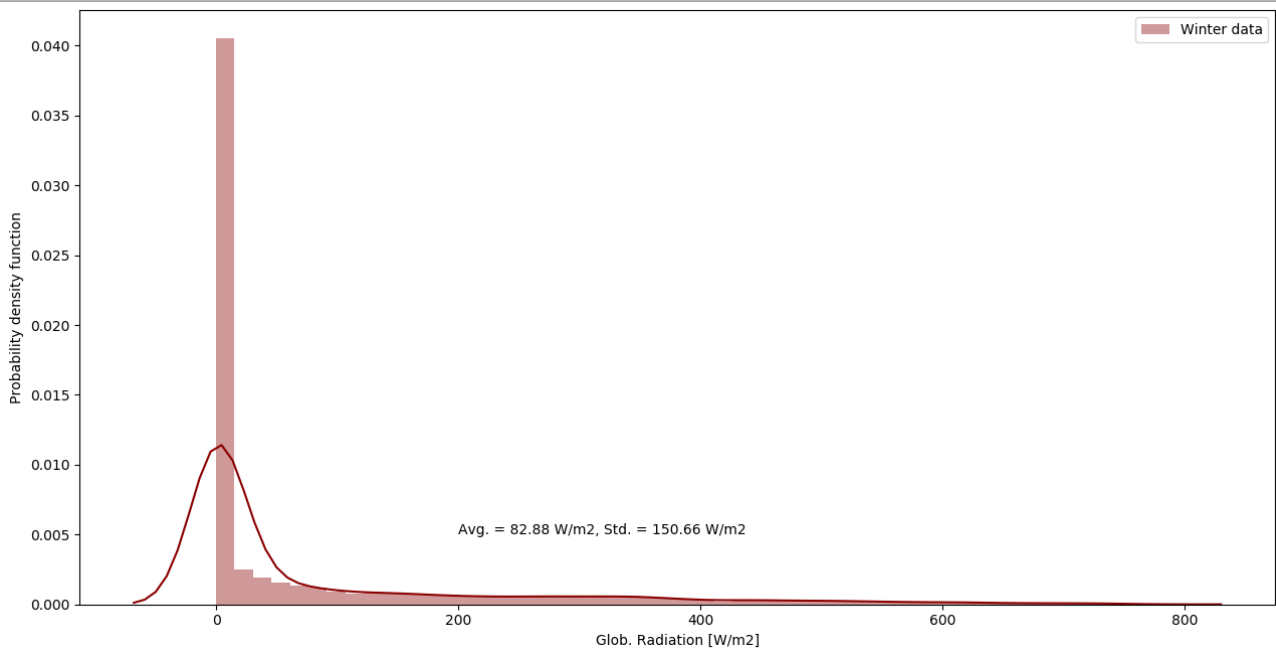


Figure 33: Probability distribution function of the Horizontal global solar radiation, considering winter season values from 2016 to 2019. Highlighting value average and standard deviation.

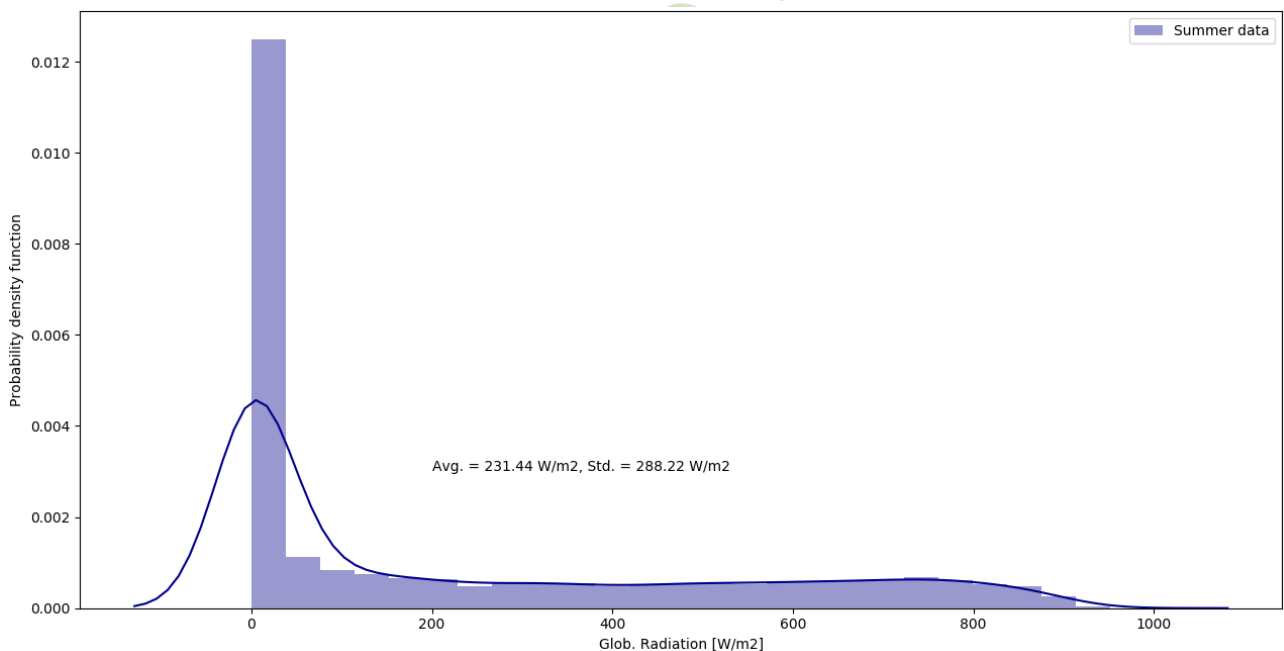


Figure 34: Probability distribution function of the Horizontal global solar radiation, considering winter season values from 2016 to 2019. Highlighting value average and standard deviation.

In particular, these analyses show that for winter there are very small quantities of potential solar gains to reduce the need for heating. And, that the variance of solar radiation is rather high given such large standard deviation values. This could be a result of cloudiness (sky coverage), which unfortunately was not reported by any of the weather stations to use as corroboration.

2.2 Inhabitants thermal sensation

There are few indexes dedicated to integrating few of the weather parameters to understand the proper sensation of people outdoors. However, most of them require rather extensive in-situ surveys that feed the model with several measured quantities. Fortunately, indexes such as the UTCI required rather common parameters to establish a preliminary analysis of the pedestrian's sensation of its surroundings.

As there is very limited information on how the occupant is exposed to radiation, and what are the surface temperatures of the area surrounding the weather station of *v. Juvara* the mean radiant temperature has been assumed as equal to air temperature.

However, before using the calculated UTCI values, an even more preliminary analysis was performed to acknowledge the overlap of undesirable conditions.

a. Confluence of risk conditions

As the risk of a high-temperature perception will only be valid, an analysis was performed with the data from *v. Juvara* weather station for the year of 2019. To study the confluence or co-occurrence of disadvantageous conditions in terms of temperature, relative humidity, wind speed and solar radiation a simple Boolean and weighting analysis was performed.

That is, for every hour of the year the condition of each parameter was verified, and if so, this was allocated with a certain risk weight according to their influence on thermal stress, and all the weights were summed for every single hour of the year. For instance, as the temperature is perhaps the most relevant parameter it was given a weight of 0.4 when it was above 26°C; then, solar radiation was given a value of 0.3 when it went above 300 W/m²; and wind speed and relative humidity were given a weight of 0.15 each if the wind speed was below 2 m/s and RH was outside the 30-70% range.

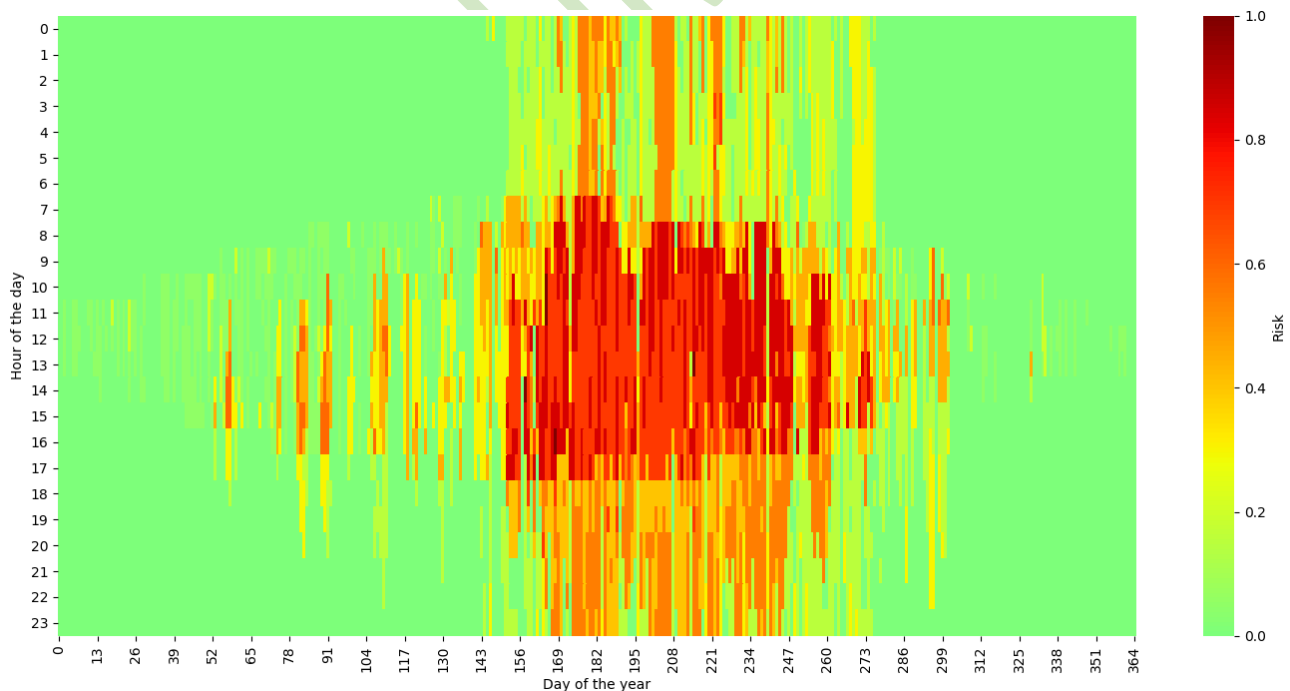


Figure 35: Degree of risk from values monitored in 2019 at *M. v. Juvara*, based on the confluence of disadvantageous weather conditions, related to the SLOD of increasing temperatures. Every parameter has been given a weight: 0.4 for temperatures > 26 °C (< 18 have been set as -0.4); 0.3 for radiation > 300 W/m²; 0.15 for wind speed < 2 m/s; and, 0.15 for relative humidity > 70% or < 30%.

In brief, if the sum of risk weights reached 1 for that particular hour of the year, all undesirable conditions were met simultaneously (highest risk). Results have been plotted in Figure 35.

From Figure 35, it can be noted that although summer has a concentration of most of the risky conditions, in some days of winter/mid-season (e.g. day 55, February) some very warm perception could be achieved. Also, it is worrying that during summer even in very late or early hours of the day, when the sun might not be above the horizon, risky conditions prevail.

b. UTCI

Following the calculation methodology described by Bröde et al. (2009), the values for UTCI were computed and plotted for a single year using data coming from the *v. Juvara* weather station. These values were plotted in Figure 36, giving a color equal to the risk categories established and previously presented in Figure 3.

The results for UTCI in Figure 36 at glance, resemble the values presented in Figure 35; however, as the UTCI did not consider solar radiation (mean radiant temperature = air temperature), it is reasonable that the risky situations identified during winter/spring or winter/autumn with the previous analysis did not arise.

Moreover, the high notorious risk at early and late hours during summer represents a huge risk in terms of *increasing temperatures* SLOD. That is because of a constant thermal stress to which people are being subjected, which can generate an increase in mortality, especially in vulnerable people (Jackson et al. 2010; Gasparini et al. 2015).

The issue of vulnerable population will be later assessed in Deliverable D2.2.5.

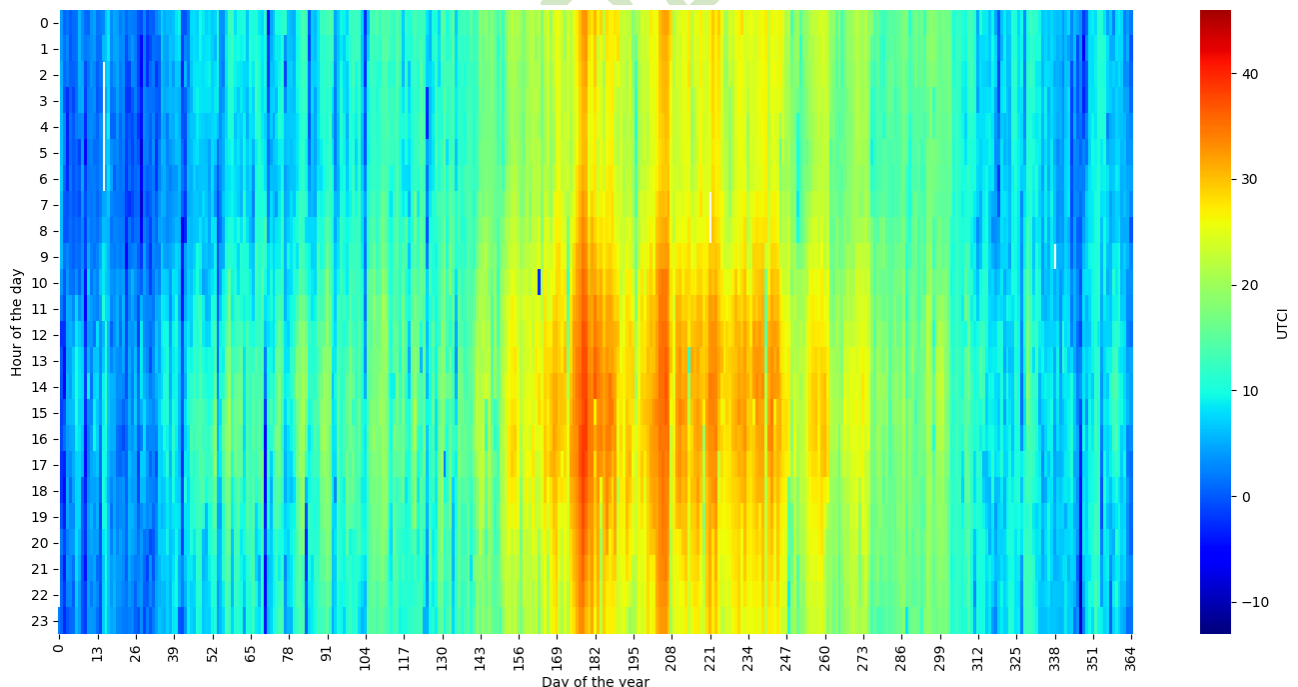


Figure 36: Degree of Thermal stress expressed in UTCI, based only on the values for 2019 from *M. v. Juvara* of air temperature (assumed equal to mean radiant temperature), relative humidity and wind speed.

2.3 Indoor air conditioning effects

For solving discomfort or risky conditions indoors, and in some cases outdoor (e.g. outdoor heaters or water mist spray for cooling), plant systems are designed, sized and installed. The use of these plant systems for delivering proper thermal conditions has proven to generate larger pollutant concentrations within dense areas (Batterman and Burge 1995; Wang et al. 2016). Therefore, a preliminary analysis was carried out in order to correlate this behavior with the pollutant entrapment and concentration.

The values retrieved from *M. v. Juvara* for 2019 have been utilized for computing Heating and Cooling degree hours (HDH and CDH) (**Errore. L'origine riferimento non è stata trovata.**), given that these are calculated based on the daily average of external air temperature and that in Figure 5 most of the stations have shown a rather similar trend (weather station selection). And the values from *M. Citta Studi* for air pollutant was used as it is the closest Air Quality station with sufficient data for the same analysis period.

HDH and CDH were computed by setting a heating base temperature of 26 °C and a cooling base temperature of 20 °C, based on the wider range of operative temperature setpoints for building category B indoor spaces (e.g. *Single Office, Landscape Office, Conference room, Auditorium, Cafeteria/restaurant, Classroom*) (EN-ISO-7730 2005).

When comparing **Errore. L'origine riferimento non è stata trovata.** and **Errore. L'origine riferimento non è stata trovata.**, it is interesting to see how the O₃ concentration follows the trend of air temperature meaning that the O₃ production could be related to the use of cooler air conditioning or of the chemical reaction of certain substances with higher temperature and solar radiation. Moreover, ammonia, black carbon, PM_{2.5} and PM₁₀ follow the trend of heating degree days, meaning that these could be correlated to the emissions of buildings heating plant systems.

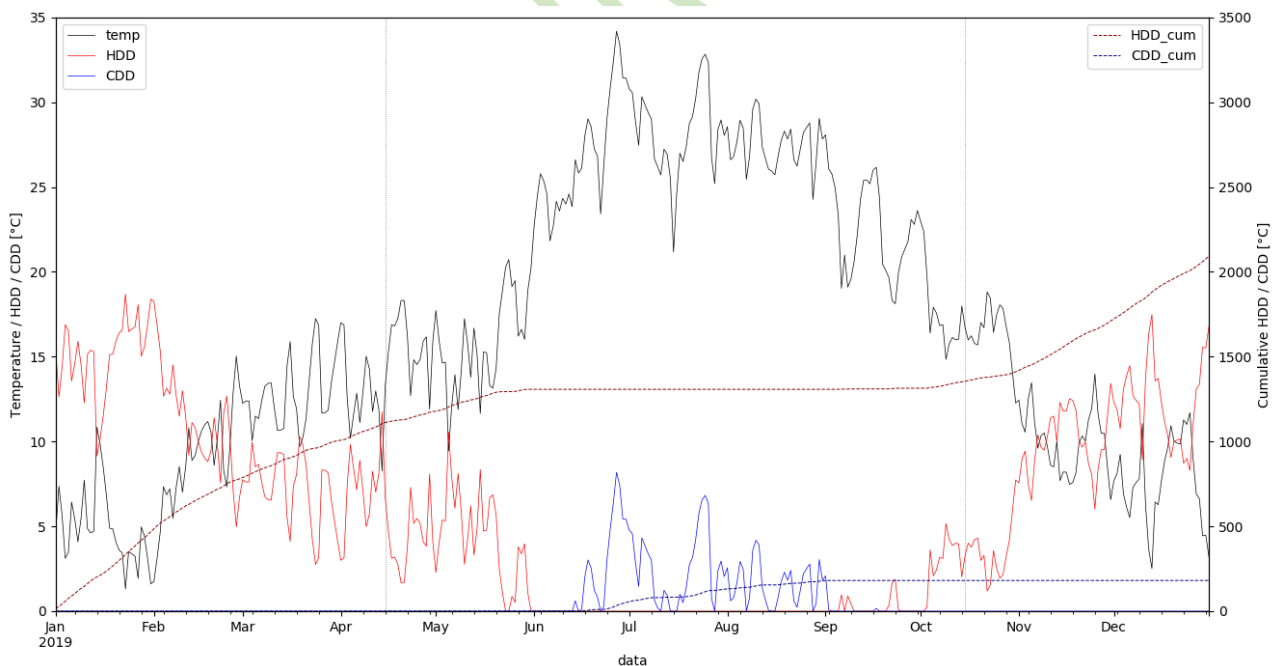


Figure 37: Daily average of air temperature from *M. Juvara* weather station for 2019, calculating daily heating and cooling degree day, and the cumulative degree days. Grey vertical lines have been drawn to show the beginning (right, Oct. 15) and end (left, Apr. 15) of the municipality's heating season.



BE S²ECURE

(make) Built Environment Safer in Slow and Emergency Conditions through behavioral assessed/designed Resilient solutions

Grant number: 2017LR75XK

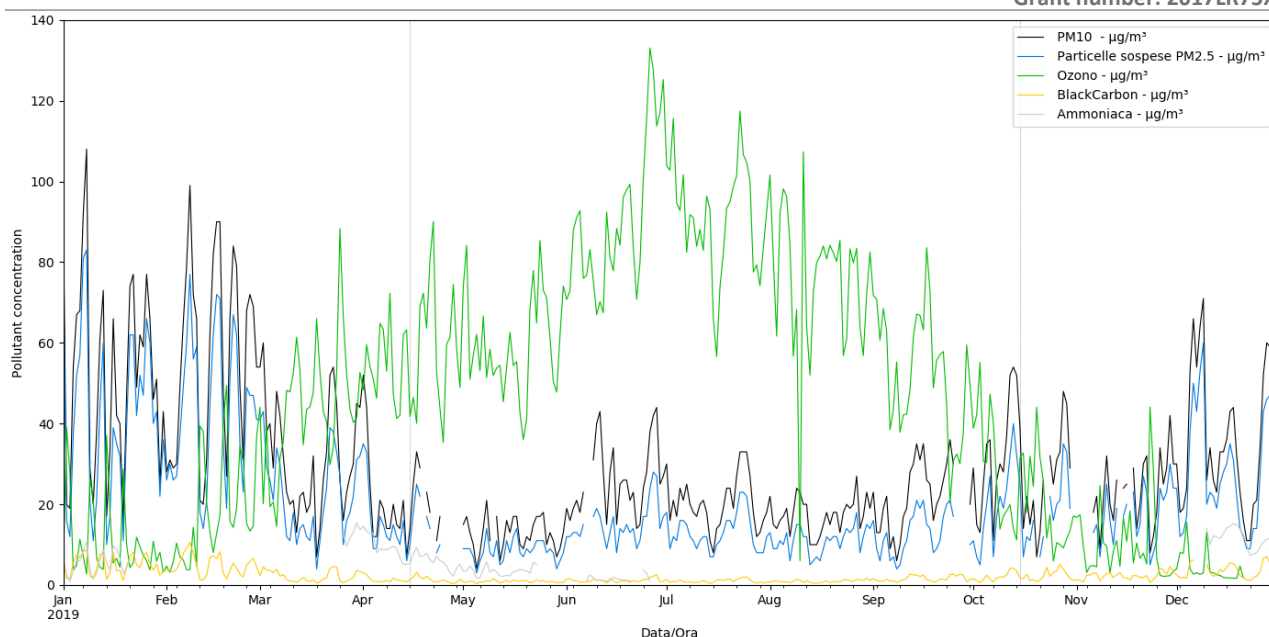


Figure 38: Daily average of pollutant concentration from M. Pascal Città Studi weather station for 2019. Grey vertical lines have been drawn to show the beginning (right, Oct. 15) and end (left, Apr. 15) of the municipality's heating season.

3. Conclusions

The report provides a comprehensive analysis of the weather data available on the Open Data Lombardia portal (Regione Lombardia). Unfortunately, these data are not always complete and reliable, therefore a careful data cleaning must be accomplished before carrying out the historic data analyses. These datasets are collected through a set of sensors contained in 10 weather stations around Milano. Only 5 of them have provided reliable data for the considered analysis period 2016-2019.

Once the analyses for the whole city of Milan have been accomplished, an insight has been done on the closest central to the case study area, located in the Città Studi neighborhood. This allows acquiring a good knowledge of the trends related to the air temperature, precipitation, Relative Humidity, wind velocity and global radiation. Also, it enabled a gross correlation of this gained knowledge, with the characteristics of the built environment previously described in D2.1.2; identifying which conditions are related to rather favorable or unfavorable weather conditions for the pedestrians immersed.

The report deepens on an analysis of these parameters on the previously selected area, to understand to what extent the weather conditions could be of significant *increasing temperatures* SLOD risk. The work concludes by combining the analyses accomplished in a synthetic indicator allowing to compare the joint impacts of the considered phenomena on the users' comfort (§ 2.2). This approach can be used together with the Air Quality Index (AQI) presented in the D2.2.2 for assessing the main weather and air pollution factors, affecting the users' health and comfort.

For example, the weather conditions might force the context to use certain appliances (e.g. heating or cooling systems) that increase air pollutants concentration. Even just the change of behavior given the extreme conditions, such as the increase of use of the personal automobile avoiding walking and biking.

4. References

- ARPA Lombardia Dati e Indicatori. <https://www.arpalombardia.it/Pages/Ricerca-Dati-ed-Indicatori.aspx#>
- Batterman SA, Burge H (1995) HVAC systems as emission sources affecting indoor air quality: a critical review. *HVAC&R Res* 1:61–78
- Bröde P, Fiala D, Blazejczyk K, et al (2009) Calculating UTCI equivalent temperature. *Environ Ergon* XIII, Univ Wollongong, Wollongong 49–53
- Cheng V, Ng E (2006) Thermal comfort in urban open spaces for Hong Kong. *Archit Sci Rev* 49:236–242
- EN-ISO-7730 (2005) ISO 7730:2005
- Gasparri A, Guo Y, Hashizume M, et al (2015) Mortality risk attributable to high and low ambient temperature: A multicountry observational study. *Lancet*. [https://doi.org/10.1016/S0140-6736\(14\)62114-0](https://doi.org/10.1016/S0140-6736(14)62114-0)
- Jackson JE, Yost MG, Karr C, et al (2010) Public health impacts of climate change in Washington State: Projected mortality risks due to heat events and air pollution. *Clim Change* 102:159–186. <https://doi.org/10.1007/s10584-010-9852-3>
- Lyons PR, Arasteh D, Huizenga C (2000) Window performance for human thermal comfort. *Trans Soc Heat Refrig Air Cond Eng* 106:594–604
- Regione Lombardia Open Data Regione Lombardia | Open Data Regione Lombardia | Open Data Regione Lombardia. <https://dati.lombardia.it/>. Accessed 26 Mar 2020
- Wang F, Meng D, Li X, Tan J (2016) Indoor-outdoor relationships of PM_{2.5} in four residential dwellings in winter in the Yangtze River Delta, China. *Environ Pollut* 215:280–289